October 2023

Regulated Intramembrane Proteolysis by M82 Peptidases: The Role of PrsS in the Staphylococcus aureus Stress Response

Baylie M. Schott
University of South Florida

Regulated Intramembrane Proteolysis by M82 Peptidases: The Role of PrsS in the *Staphylococcus aureus* Stress Response

by

Baylie M. Schott

A thesis submitted in partial fulfillment
of the requirements for the degree of
Master of Science
Department of Molecular Biosciences
College of Arts and Sciences
University of South Florida

Major Professor: Lindsey N. Shaw, Ph.D.
Prahathees Eswara, Ph.D.
Zhiming Ouyang, Ph.D.

Date of Approval:
October 24th, 2023

Keywords: M82, PrsS, proteolysis, DNA-damage, regulated intramembrane proteolysis

ACKNOWLEDGMENTS

To my committee, thank you all for taking the time to be a part of this journey with me. I'm incredibly grateful for your insight and guidance. To my parents, thank you for endlessly supporting me. You both have encouraged me beyond words and have celebrated my success at every benchmark. I couldn't ask for a greater gift in this life than you two. To Ryan, thank you for staying up countless hours with me practicing presentations, studying, and listening to me re-write the same paragraph one thousand times. You are the greatest partner one could ever have through this journey, and I'm so lucky to have you by my side. To my lab, in the greatest cliché, you all have become like family to me. Thank you, Dr. Shaw, not only for the way you have inspired me to be a better scientist, a better person, a better friend, and a better colleague, but also for the community you've created within this lab. I'm certain if I'd have been anywhere else, I wouldn't have followed it through. The way that you believed in me, even at the hardest times to do so, is something I will never forget. Nate, thank you for your patience and mentorship throughout this experience. You taught me so much, and you did so with grace. You were always able to put yourself in a graduate student's shoes, and I truly admire you for that. MEJ, thank you for your unwavering kindness, friendship, and snacks that you've provided me over the last two years. You're an amazing person and an incredibly gifted scientist, and I can't wait to see where life takes you. You've given so much to this process and the people around you, and I can't express enough what an absolute light you are to have around. Jessica, thank you for your support and guidance. You have always made

me feel that my questions were valuable, which is how I know you'll be an exceptional mentor to others. You are one of the hardest workers I have ever met, and it has deeply inspired me. Emily, thank you for your kindness and understanding. You gave me so much patience and acceptance when I first started here, and I'll always remember how welcome you made me feel when I needed it most. Emilee, you have not only been one of the most amazing friends I've made throughout this journey, but you've also contributed so much to this project. I cannot thank you enough for being so dependable when it comes to both your friendship and your work. Thank you for supporting me through all my big events, and always keeping me caffeinated. You are, without a doubt, one of the most talented scientists I know. Brendan, I could not have made it through this without you. You are truly a one-of-a-kind friend and have contributed so much to my time here. You have shown up for me and lifted my spirits a dozen times, and I'm so grateful for you. Julia, I can honestly say that you make every single day fun. You are, unironically, people's greatest cheerleader – it's a true gift to have someone by your side who celebrates your wins and "Justice for Baylie"s through your losses. You are a brilliant scientist and friend, and I'm really going to miss you. Rachel, you are such a genuine and honest person and I admire that about you so much. You have always made me feel included, and you've been such a good sport through all my pranks. You have provided me with endless laughs and Hello Pandas, and I can't wait to see your success. You are incredibly smart, and a wonderful cat mom.

This thesis is dedicated to my dog Toby, who has been my greatest companion from middle school to graduate school.

TABLE OF CONTENTS

LIST OF TABLES

LIST OF FIGURES

ABSTRACT

Staphylococcus aureus is a major threat to human health, which is only exacerbated by its resistance to methicillin and other frontline antibiotics. Consequently, annual hospitalizations resulting from methicillin-resistant *Staphylococcus aureus* (MRSA) have been recorded in the hundreds of thousands for decades. However, the global impact of this opportunistic pathogen cannot solely be attributed to its antibiotic resistance, as *S. aureus* is also an expert at adapting to host conditions and responding to external stress. Here we attempt to gain a better understanding of a *S. aureus* factor that aids in circumventing such external insult - PrsS - a membrane protease that governs the response to DNA damage and cell-wall targeting antibiotics. We began by performing a structure-function analysis of PrsS, exploring its 8 transmembrane domains (TMD) and 4 conserved protease motifs. Here, we found seven residues within TMDs 4-7 that were necessary for PrsS function, all of which are in conserved protease motifs. We also investigated the function of the N-terminal extension of PrsS as well as its C-terminal tail (CTT), finding the first five amino acids in the CTT to be imperative for responding to DNA damage. Further to this, we evaluated the transcriptional regulation of *prsS*, identifying multiple factors modulating its expression. Interestingly, *prsS* expression is repressed by SigB, PurR, HrcA, SarZ, and GlcT, and activated by Rsp. Notably, SrrA was found to repress *prsS* expression, but only in the presence of MMS. Finally, we used N-terminomic methodologies to identify potential substrates of PrsS. A wealth of important proteins were

found to be cleaved by PrsS, including ribosomal subunits, the cell division protein FtsZ, and a cryptic membrane protein of unknown function. In summary, we have generated important new knowledge, not only on PrsS' role in *S. aureus* virulence, but more broadly on a protease family that is conserved across all kingdoms of life.

CHAPTER ONE: INTRODUCTION

Methicillin-Resistant *Staphylococcus aureus*

The global impact of *Staphylococcus aureus,* one of the most detrimental pathogens in the history of human health, is often attributed to its antibiotic resistance. However, in the 1940s *S. aureus* infections were once treatable with a simple penicillin regimen [1]. Penicillin-resistant *Staphylococcus aureus* emerged shortly after the clinical introduction of this antibiotic, and the development of alternative therapeutics became a pressing concern [1]. Methicillin then followed as the primary therapy used to treat *S. aureus* infections in 1959 [1,2], and the first documented case of methicillin-resistant *S. aureus* (MRSA) was observed the following year [1]. This sparked the emergence of a worldwide health crisis, as it seemed this pathogen was always one step ahead of human medicine.

S. aureus rapidly developed resistance to these drugs by modulating the process by which they target this pathogen [32]. β-lactam antibiotics like penicillin and methicillin function by forming covalent bonds within the transpeptidase domain of penicillin-binding proteins (PBPs), inhibiting peptidoglycan synthesis [31]. *S. aureus* evades β-lactam inhibition by expressing an alternate penicillin-binding protein, PBP 2a, or by secreting β-lactamases resulting in antibiotic degradation [31]. It's widely accepted that the prior use of penicillin created selective pressure for *S. aureus* strains possessing these β-lactam resistance mechanisms to persist, facilitating the rapid development of MRSA [1,2].

Recently it's been estimated that MRSA infections are responsible for 300,000 annual hospitalizations in the United States alone [3]. While these numbers are rising, clinical isolates obtained from these patients are becoming more diverse. MRSA was once considered to be a predominantly hospital-acquired infection, but a dramatic shift has been observed in the last two decades [4]. This sudden change has encouraged further studies characterizing the two distinct MRSA strains.

Hospital and Community-Acquired MRSA

Methicillin-resistant *Staphylococcus aureus* infections are categorized into two unique types: hospital-acquired MRSA (HA-MRSA) and community-acquired MRSA (CA-MRSA). While HA-MRSA has historically comprised a vast majority of clinical isolates, in just 16 years, the presence of community-acquired MRSA isolates jumped from 0% to 24% [33]. While HA- and CA-MRSA each have unique genetic identifiers, their primary differentiation is determined by the patient's history. MRSA infections that present in a patient prior to 48 hours of hospitalization are considered CA-MRSA, and these cases often occur in generally healthy adults [1]. HA-MRSA is identified in patients who have had prior surgeries, extended hospital stays in the preceding year, or have been in the hospital for longer than 48 hours at the time of infection [1].

However, there are more complex genetic distinctions between HA- and CA-MRSA that can determine their antibiotic resistance. Each of these strains has antibiotic resistance traits associated with their staphylococcal cassette chromosome *mec* (SCC*mec*) types. SCC*mec* is a mobile genetic element with a varied cassette of genes that impact overall

pathogenesis [6]. This cassette contains the *mecA* gene which is responsible for resistance to β-lactam antibiotics including penicillin and methicillin, proving to be extremely relevant in current drug discovery efforts [6]. Importantly, many SCC*mec* elements contain multiple different variations of the *mecA* gene, resulting in the divergence of antimicrobial resistance in MRSA [8]. SCC*mec* cassettes also contain variations in their respective *ccr* gene complexes, which encode for specific recombinases that facilitate the mobility of this genetic element [25,26]. These variations in the *mec* and *ccr* complexes primarily define each SCC*mec* type [25]. For example, SCC*mec* types II and IV both contain *ccr* gene complex 2, however, they vary in *mec* gene complexes, containing A and B respectively [25]. On the other hand, SCC*mec* types I and IV each contain the B *mec* gene complex, but they have variations in their *ccr* gene complexes, containing complexes 1 and 2 respectively [25]. HA-MRSA frequently also possess resistance to non-β-lactam drugs, aligning with their contained SCC*mec* types I, II, and III [5]. Alternatively, CA-MRSA contain SCC*mec* types IV and V and are often more susceptible than HA-MRSA to treatment with antimicrobials such as gentamicin, tetracycline, and rifampicin [1,27]. Some examples of CA-MRSA are only resistant to β-lactam antibiotics [1].

Not only do genetic analyses tell us about these strain's antimicrobial resistance patterns, but they can also give us insight into how they'll interact with the host immune system. The Panton-Valentine Leukocidin (PVL) toxin, an *S. aureus* virulence factor, is another differing genetic component of HA- and CA-MRSA strains. A 2016 study showed that PVL presence alone can be enough to discern whether an infection is HA- or CA-MRSA [7,8].

CA-MRSA commonly contain the *lukS* and *lukF* genes encoding the PVL toxin, which destroys white blood cells resulting in increased virulence [8]. HA-MRSA does not traditionally have these genes, which are necessary to produce the PVL toxin, and therefore does not attack the immune system by the same processes as PVL-positive CA-MRSA [8,9]. HA-MRSA is predicted to depend more on immune-evasion tactics, whereas CA-MRSA takes a more aggressive approach against the immune system through toxin production [9]. These are just a few of many genetic components playing a major part in *S. aureus'* antibiotic resistance and interaction with host immune responses. However, another vital contributor to *S. aureus* pathogenic success stems from the organism's highly adaptive nature to conditions within the host.

Host-Condition Adaptability

S. aureus, unlike many other bacteria, can survive in nearly every niche of the human body [10]. This pathogen is responsible for highly diverse infection sites and severities, including skin and soft-tissue infections, osteomyelitis, endocarditis, and in some cases deadly septicemia [10]. By deploying highly specialized methods of gene regulation, *S. aureus* can colonize various types of host tissues within the heart, lungs, bones, blood, and skin of infected patients [28, 29]. As these distinct environments have unique cellular stressors associated with immune response, temperature, pH, oxygen availability, and nutrient starvation, *S. aureus* must respond accordingly to survive [11, 30]. A major way that *S. aureus* adapts and responds to host conditions is through the signaling pathway of two-component systems.

There are 16 two-component systems (TCS) that *S. aureus* uses to respond to conditions in the host environment [34]. WalRK is the only TCS that is essential for growth, but the deletions of many TCS exhibit reduced survival in the presence of external stressors such as antibiotics, oxidative stress, and high temperatures [34]. TCS respond to conditions in the host through the phosphorylation of a histidine kinase receptor upon sensing stress signals [35]. This phosphate group is then donated to a response regulator, which can bind to promoters of target genes and modify their expression [35]. One primary example of TCS gene regulation in host conditions is found in the LytRS system [35]. In an active immune response, host cells release cationic antimicrobial peptides that bind to bacterial membranes and destabilize them [35]. LytS is autophosphorylated in response to CAP-induced stress signals and transfers this phosphate group to LytR [35]. This response regulator then binds directly to the promoter of *igrAB,* upregulating its expression and inhibiting cell lysis [35]. Ultimately, TCS are just one major signaling pathway used by *S. aureus* to alter gene regulation and modulate external stress within the host environment. However, this pathogen also utilizes sigma factors to influence gene expression, facilitate cell survival, and respond to stress.

Sigma Factors in *S. aureus*

Generally, bacterial sigma factors function through their continual binding and release from RNA polymerase (RNAP) - this process is known as the sigma cycle [13]. Sigma factors facilitate promoter recognition and proper positioning of the holoenzyme, allowing RNAP to initiate transcription [12,13]. Thus, specific gene transcription is dependent on

the sigma factor bound, and this specificity can be used to modulate gene expression in both a housekeeping and stress-dependent manner [13].

Unlike many other gram-positive bacteria, *Staphylococcus aureus* only encodes four sigma factors [12]. This pathogen contains a primary housekeeping sigma factor: σ^A, which is necessary for growth and facilitates response to general nutritional and antibiotic stress [12]. *S. aureus'* σ^A is homologous with the primary sigma factors of *B. subtilis* and *E. coli,* and it recognizes homologous promoters between each of these organisms [12]. This high level of structural and functional conservation is necessary, as this housekeeping sigma factor is essential for bacterial cell survival. Importantly, σ^A is responsible for most promoter recognition and gene transcription in the cell, including the transcription of the alternative sigma factors in *S. aureus* [12].

Like σ^A, the *S. aureus* alternative sigma factor σ^B contains homologs in other gram-positive organisms as well [36]. σ^B is the most influential alternative sigma factor in *S. aureus* and has been described to assist in the transcription of approximately 200 genes, as well as regulating its own expression [37]. This widespread influence on gene regulation ultimately aids the cell in responding to several different host conditions including nutrient starvation, excessive heat, acidic pH, stationary phase associated stress, high salt content, and nitrosative stress [12]. Additionally, σ^B actively contributes to host-immune evasion by initiating a switch in *S. aureus* from highly aggressive behavior to a metabolically inactive small colony variant phenotype, facilitating long-term intracellular persistence [38]. This alteration in phenotype requires the silencing of Agr

and SarA, two of the most important *S. aureus* virulence regulators, for σ^B to take over during chronic infection [38]. This transfer of expression highlights the importance of σ^B in both stress response and host infection dynamics.

S. aureus possesses two other alternative sigma factors that contribute to survival in the host as well. σ^H is observed to be associated with cytoplasmic stress in the presence of a phage 11 infection and is predicted to be a factor in lysogenic state stabilization [12]. However, the primary importance of this alternative sigma factor arises from its role in *S. aureus* competence [39]. While *S. aureus* is not naturally competent, the ability to develop competence is an important mechanism during times of energy-associated stress [39]. σ^H overexpression is induced when *S. aureus* cells enter a state of respiratory distress, often stimulated by the natural host production of reactive oxygen species (ROS), that force this pathogen to use fermentation as an energy-alternative [39]. Due to the low efficiency of fermentation-based energy acquisition, an increase in glycolytic flux is required to maintain normal cellular processes [40]. Ultimately, in the σ^H mutant *S. aureus* struggles to upregulate the necessary genes to facilitate competency, leaving the cell at risk for reduced survival in host-cell induced ROS conditions [39]. However, σ^B is capable of overexpressing competency genes and mediating these effects, further highlighting its vast importance in the host environment [39].

This alternative sigma factor-regulated transcription of response genes, in addition to the use of TCS and transcription factors, is a way for *S. aureus* to circumvent adverse conditions during infection. *S. aureus* contains one additional sigma factor that aids in

these efforts; however, this alternative sigma factor is unique in that it falls under a further subcategory of alternative sigma factors - extracytoplasmic function sigma factors.

Release of ECF Sigma Factors by Regulated Intramembrane Proteolysis

Following closely behind one and two-component systems in terms of abundance, extracytoplasmic function (ECF) sigma factors are one of the most important facilitators of signal transduction in bacterial cells and are induced by the presence of an extracytoplasmic stress signal [15]. Typically, in the presence of external stress, an anti-sigma factor is cleaved from the ECF sigma factor by two separate proteolytic events, allowing this ECF to facilitate the transcription of stress-response genes [17]. This general process is known as regulated intramembrane proteolysis - a pathway that admits external signals into the cell membrane by cleaving or degrading a transmembrane protein, altering gene transcription in times of stress [17,19,20]. Proteolysis is innately a very quick process, facilitating a quick response in these adverse conditions [19]. However, not all ECF sigma factors are released by regulated intramembrane proteolysis.

Within the last two decades, our group discovered an ECF sigma factor in *S. aureus*, σ^S. This ECF sigma factor is important for responding to cell lysis, starvation, and lengthy exposure to adverse temperatures, and has recently been discovered to facilitate protein expression of opposing modulators acting on its own mRNA stability [41,42]. Additionally, the σ^S mutant has shown increased sensitivity under oxidative stress conditions, DNA damage, and cell-wall targeting antibiotics, suggesting the importance of σ^S-mediated gene regulation in circumventing these external threats [23]. In murine models of septic

arthritis, σ^S has also been shown to be necessary for full *S. aureus* virulence [16]. While there's no question that this ECF sigma factor aids *S. aureus* in mediating adverse host conditions, the mechanism by which σ^S is regulated remains elusive. By investigating both traditional and non-traditional mechanisms that facilitate the release of ECF sigma factors, there is potential to uncover additional insight into σ^S regulation.

One of the most well-characterized examples of regulated intramembrane proteolysis can be found in gram-negative *Escherichia coli. E. coli* contains an ECF sigma factor, σ^E, which aids the cell in mediating cell envelope and heat-associated stress [20]. This sigma factor is responsible for recognizing roughly 20 different gene promoters and is even responsible for regulating its own secondary promoter [20]. In the absence of extreme heat or cell-envelope stressors, σ^E is natively bound by the anti-sigma factor RseA [20]. To release this ECF sigma factor, two cleavage events must occur, removing RseA [20]. Initially, DegS undergoes a conformational change into a proteolytic state and enacts site-1-proteolysis in RseA [20]. In this primary truncated state, RseA is then able to be cleaved by RseP in a site-2-proteolysis event [20]. However, even after this secondary cleavage event, RseA is still able to sequester σ^E. The final event of this regulated intramembrane proteolysis pathway occurs when ClpX forcibly removes RseA from σ^E, allowing it to bind to RNAp and initiate transcription of genes controlled by this ECF sigma factor [20]. However, as this is only an overview of a common ECF sigma factor signal transduction pathway, it's important to recognize that there are a handful of examples that diverge from the general mechanism.

Streptomyces coelicolor, a gram-positive soil bacterium, possesses an ECF sigma factor σ^E that is presumed to be activated by several cell-wall targeting antibiotics and results in the transcription of cell-wall biosynthesis genes [18]. While this relationship with external stress makes sense with what we know of ECF sigma factors, σ^E is not natively bound by an anti-sigma factor [18]. Instead, this ECF sigma factor is transcriptionally regulated, as opposed to the post-translational regulation we see with many other sigma factors of its kind. The transcription of σ^E depends partially on proteins CseB and CseC, which make up a two-component system [18]. This was verified through the observation that the *cseB* mutant strain displays no σ^E transcription [18]. Notably, σ^E is also partially self-regulated and is responsible for activating its own second promoter [18]. While this pathway in *S. coelicolor* demonstrates an unusual ECF regulation mechanism, there are certainly traditional mechanisms by which ECFs are regulated in gram-positives. *Bacillus subtilis* displays a textbook example of regulated intramembrane proteolysis in gram-positive organisms, enacted by a novel family of proteases.

Regulated Intramembrane Proteolysis by M82 Peptidases

In *Bacillus subtilis,* ECF sigma factor σ^W is responsible for the recognition of over 60 genes related to cell-envelope stress and cell-wall integrity, and its regulation mechanism is well characterized [20]. σ^W is activated by a traditional regulated intramembrane proteolysis pathway and is therefore natively bound by anti-sigma factor RsiW in the absence of an external stress signal. Activating signals, induced by alkaline shock or antimicrobial peptide-associated stress, initiate the site-1-proteolysis of RsiW by the M82 peptidase PrsW [21,23]. This primary cleavage event leaves truncated RsiW bound to σ^W

[20,21], where it is subsequently cleaved through site-2-proteolysis by RasP [21]. This process is innately regulated and incredibly quick, as RsiW immediately becomes a substrate for RasP in its truncated state [20]. These cleavage events directly lead to the release and ultimate activation of ECF sigma factor σ^W, which can then facilitate gene transcription and stress response. Interestingly, a homolog of the M82 protease PrsW, responsible for this site-1 proteolytic cleavage event in *B. subtilis,* is also found in *Clostridium difficile.*

In *C. difficile,* the M82 peptidase PrsW induces the degradation and proteolytic cleavage of anti-sigma factor RsiT through site-1 proteolysis [22]. Unlike traditional regulated intramembrane proteolysis mechanisms, this pathway in *C. diffiicile* only appears to require a single cleavage event [22]. This site-1 proteolysis ultimately results in the release of ECF sigma factor CsfT and transcription of stress response genes associated with the CsfT operon [22]. *Clostridium difficile* CsfT, and thus PrsW, facilitate stress response to cell-wall biosynthesis inhibitors and peptidoglycan destabilization [22]. Interestingly, this M82 peptidase is necessary for full pathogenic success in *Clostridium difficile*, as the PrsW mutant resulted in 30-fold decreased virulence in hamster models [22].

Following the discovery of the lone ECF sigma factor σ^S, our group discovered a PrsW homolog in *S. aureus* denoted PrsS [23]. While no anti-sigma factor has been identified confirming a regulated intramembrane proteolysis pathway between σ^S and PrsS, evidence suggests that there is a relationship between the two [23]. PrsS exhibits a

striking similarity to σ^S in terms of DNA damage, oxidative stress, and cell-wall targeting antibiotic sensitivities, as well as its increased expression in the presence of these external stressors [16, 23]. Like σ^S, PrsS has proven to be necessary for full virulence in *S. aureus,* as the *prsS* mutant exhibits reduced survivability in murine infection models [23]. Additionally, this novel protease has been observed to be necessary for survival in whole human blood, suggesting its relevance in *S. aureus* bloodstream infections [23]. PrsS also mirrors the increased expression previously seen in σ^S observed in murine macrophages and human serum, highlighting a potential cooperative effect in these specific host factors [16,23]. By addressing the proteolysis pathways of two characterized M82 peptidases and the unknown pathway of a third, several questions arise regarding the structural importance of homologous regions within this protease family.

M82 Peptidase Structure

The M82 peptidases are a membrane-associated family of proteins, with both conserved and variable regions that have been implicated in their respective functions. Each of these proteases contains four conserved protease motifs and 5 conserved transmembrane domains, although they are present within slightly different regions of these proteases. In *S. aureus* PrsS, conserved protease motifs are all contained within transmembrane helices (TMH) 4-7. However, in *B. subtilis* PrsW and *C. difficile* PrsW, the conserved transmembrane domains align with TMH 3-6 [45]. There are no known protease motifs in TMHs 1, 2, 3, or 8 of PrsS, correlating with *B. subtilis* PrsW and *C. difficile* PrsW TMHs 1, 2, and 7 [45].

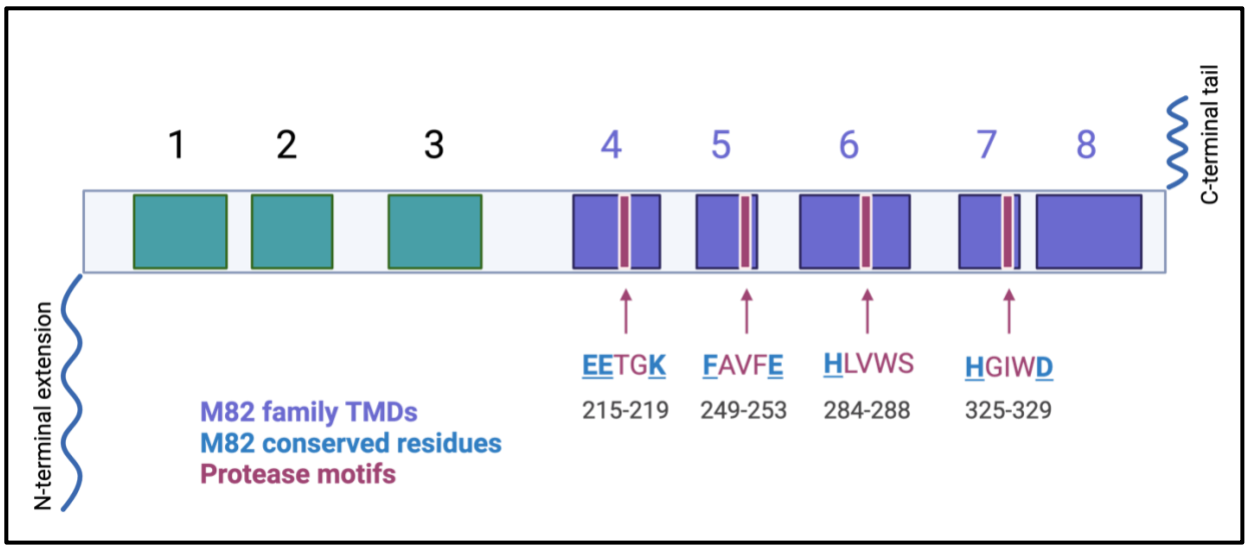

Figure 1. M82 conservation in PrsS. A model of PrsS is used to display the conserved M82 peptidase regions. Transmembrane domains are depicted in purple. Conserved residues are depicted in blue. Protease motifs are depicted in red.

The first protease motif, contained in PrsS TMH 4 and denoted EExxK, contains double glutamic acid residues that have been determined important for functional stress response in PrsS [21], and important for PrsW-mediated σ^W activation in *B. subtilis* [23]. The histidine in the third motif, contained in PrsS TMH 6 and denoted Hxxx, has been evaluated and deemed necessary for PrsW to activate σ^W expression as well, as seen in β-galactosidase assays with transcriptional fusion reporters [21]. The M82 peptidases not only possess structural conservation within themselves, but they also contain multiple conserved regions and basic frameworks found in eukaryotes, prokaryotes, and archaeal species of metalloproteases.

Structural Comparisons of the M82 and G5 Peptidase Families

When structurally defining the M82 peptidase family, it would be remiss to not discuss the membrane-embedded metalloproteases (MEM) superfamily. This superfamily is

predicted to play a role in protein secretion and peptide modification, primarily in plants and bacteria [20, 24]. Under the umbrella of this MEM superfamily, a subfamily exists called the G5 peptidase family [24]. The G5 peptidases, previously referred to as the CAAX Proteases and Bacteriocin Processing-enzymes (CPBP), retain homologs across every kingdom of life, including the M82 peptidases [20,24].

The G5 family contains four conserved C-terminal transmembrane domains, all of which are conserved across the M82 peptidases, and three protease motifs [24]. The first protease motif of the G5s, denoted EExxxR, contains double glutamic acid residues followed by a conserved arginine [24]. We see the same double glutamic acids mirrored in the first protease motif of the M82 peptidases, however, the M82s lack this conserved arginine and instead possess a conserved lysine at the end of motif 1 [24]. Similar to findings in *B. subtilis* PrsW and *S. aureus* PrsS, these double glutamic acids have been deemed necessary for proteolytic function in the G5 peptidases, including the Rce1 protease found in *Saccharomyces cerevisiae* [21, 53]. Additionally, the remaining two protease motifs in the G5 peptidases, denoted FxxxH and HxxxN, share their first conserved residues with the M82 peptidases as well, as the histidine in G5 motif 3 is necessary for *B. subtilis* PrsW-mediated transcriptional activation of σ^W as previously described. These structural similarities indicate an evolutionary advantage passed down for generations within the MEM superfamily, and therefore must be further investigated for their relevance within the M82 peptidases. As seen from PrsS, homologs of these related protease families significantly contribute to the virulence and pathogenic success of *S. aureus,* creating high importance for M82 research.

Project Aim

It's clear that PrsS substantially aids in the survival and virulence of *Staphylococcus aureus,* and we aim to further define its contribution to pathogenic success. By evaluating this M82 protease structurally, our goal is to gain insight into which specific conserved residues and protease motifs are necessary for M82 proteolytic function, and how this function contributes to *S. aureus* regulation. While PrsS also contains structural domains lacking in fellow family members, we attempt to identify the value of these unique features and how they impact cellular stress response. Additionally, we seek to learn more about how this protease is transcriptionally regulated and analyze what factors both activate and inhibit its expression. Through analysis of *prsS* regulation, we aim to pinpoint the unique factors and conditions which influence the expression of this protease, allowing it to facilitate cell survival and protection from external stressors. Our final goal is to determine the highly specific substrates of PrsS, further defining the role of this protease in *S. aureus* post-translational regulation. By identifying these substrates, we hope to gain knowledge as to how PrsS may regulate *S. aureus* virulence factors and interactions within the host.

CHAPTER TWO: MATERIALS AND METHODS

Growth Conditions

All strains were grown at 37°C unless otherwise specified. Liquid cultures were grown in 5mL of sterile media broth in a shaking incubator at 250rpm, and agar plates were grown in a stationary incubator. All overnight cultures were incubated for 16-18 hours. *E. coli* strains were grown in LB or on LB agar plates, while *S. aureus* strains were grown in TSB or on TSA plates. Antibiotics were used when necessary to retain plasmids at equivalent concentrations in both liquid and agar media as follows: *E. coli* – Ampicillin at 100µg/mL; *S. aureus* – Tetracycline at 5µg/mL, Chloramphenicol at 10µg/mL, Erythromycin only at 5µg/mL in liquid cultures, Erythromycin at 5µg/mL and Lincomycin at 25µg/mL on agar plates. When necessary, cultures were synchronized by subculturing 50µL of overnight culture into 5mL of fresh media (1:100 dilution) containing the appropriate antibiotic and grown in a shaking incubator at 37°C for 3h. Cultures were then standardized to an OD_{600} of 0.05 unless otherwise specified, in fresh media containing the appropriate antibiotic and grown in a shaking incubator until reaching the targeted growth phase.

Cloning into *E. coli*

These methods are derived from an unpublished cloning protocol by N.J. Torres.

Using aqueous, wild-type DNA, the desired gene or promoter of choice was PCR amplified. Traditional PCR mixtures included 1µL of forward primer and 1µL of reverse primer, as well as 12.5µL of a DNA polymerase enzyme of choice, and 9.5µL of sterile

water. After PCR amplification in the thermocycler, the remaining sample was loaded onto an agarose gel and run at 100V for 30 minutes. The amplified band was cut out of the gel and purified using Qiagen's gel extraction kit. Plasmid extractions were performed using Qiagen's Mini-Prep Kit. With the purified insert and plasmid DNA, separate digestion reactions were performed on each with 1.5µL of each restriction enzyme of choice, 5µL of NEB's CutSmart Buffer, and sterile water bringing the mixture up to 50µL. Samples were incubated for 30 minutes in a 37°C water bath, then the plasmid digestion was dephosphorylated with 5µL Antarctic Phosphatase Buffer and 1µL of Antarctic Phosphatase. Both plasmid and insert samples were incubated again for an additional 30 minutes in a 37°C water bath. Digestion reactions were then purified, and the insert and plasmid were then ligated together using NEB's Ligation Calculation Tool. This ligation was performed by adding either a 3:1 or 7:1 insert to plasmid ratio to 1µL of NEB's Ligation Buffer and 1µL of NEB's Ligase. Reactions were left at room temperature overnight and were then transformed into *E. coli* DH5a.

DH5a Transformations

DH5a transformations were performed by adding 10µL of the ligation reaction obtained from the initial cloning steps to DH5a competent cells. This mixture was incubated on ice for 30 minutes, heat shocked at 42°C for 45 seconds, and incubated on ice for 2 minutes. 1mL of LB was added to this sample, which was then transferred to a 15mL falcon tube where an additional 1mL of LB was added. This mixture was incubated at 37°C for 1 hour, and subsequently centrifuged at 4150rpm for 10 minutes. Cells were resuspended in 100µL of remaining LB and plated onto the appropriate media with antibiotic selection as

previously described for *E. coli.* Plates were grown overnight, and individually selected colonies were re-streaked for population density. Following this, a colony PCR could be used to investigate the presence of the desired insert (only for *E. coli)*. Colony PCRs were performed by adding a single colony from the re-streaked plate to a mixture of 1µL of both plasmid-specific forward and reverse primers, 12.5µL of GreenGo, 9.5µL of sterile water, and run on the appropriate thermocycler settings. This same PCR mixture was made, instead using empty vector DNA as a negative control. The PCR product would then be run on an agarose gel as previously described. With a band size matching the size of the insert, the re-streaked colony would be grown in liquid culture, plasmid extracted as previously described, and sequenced.

Plasmid Sanger Sequencing

Plasmid sequencing reactions were made in pairs using 600µg of extracted plasmid DNA, with 5µL of forward plasmid specific primer in one rection, and 5µL of reverse plasmid specific primer in a separate reaction. Reactions were brought up to 15µL with sterile water if needed and sent through Azenta's GeneWiz Sanger Sequencing.

RN4220 Transformations

RN4220 transformations were performed by first thawing RN4220 competent cells on ice for 5 minutes, and subsequently incubating at room temperature for an additional 5 minutes. Competent cells were then centrifuged at 5,000rpm for 1 minute, and resuspended in 50µL of a filter-sterilized, water-solubilized mixture containing 10% glycerol with 500mM sucrose. Then, no more than 1,000µg of sequence-confirmed

plasmid DNA was added to the mixture, and the entire mixture was transferred to a cuvette and electroporated. 1mL of a sterile TSB and 500mM sucrose mixture was then added to the cuvette, mixed well, and transferred to a 15mL falcon tube. This falcon tube was placed in the shaking incubator at 37°C for 1 hour, and subsequently, 100µL was plated with the appropriate antibiotic selection and grown overnight as previously described for *S. aureus.* Selected colonies were re-streaked for density and grown overnight. RN4220 colonies were then DNA extracted for PCR confirmation.

DNA Extraction of *S. aureus*

All *S. aureus* strains were DNA extracted by growing 5mL of liquid overnight culture with the appropriate antibiotic as described for *S. aureus.* Samples were centrifuged at 4150rpm for 10 minutes, and the supernatant was discarded. Pellets were resuspended in 600µL of TE buffer and added to screw cap tubes containing 0.1MM glass beads. Samples were placed in the bead-beater and run 3x at 30 seconds each. They were then centrifuged at 17,000 x g for 5 minutes. 400µL of the resulting supernatant was transferred to a new 1.5mL epi tube, where 200µL of 1.6% sarkosyl and 5µL of proteinase K were added. Samples were mixed and placed in a 60°C incubator for 1 hour. Following incubation, 700µL of phenol-chloroform was added, samples were mixed and then centrifuged at 17,000 x g for 5 minutes. 400µL was then removed from the top layer of the remaining sample and added to a fresh 1.5mL epi tube containing 500µL of isopropanol and 100µL of 3M sodium acetate. After mixing samples, they were stored at -80°C for 1 hour. Samples were then centrifuged at 17,000 x g for 10 minutes, and the supernatant was discarded. 500µL of 70% ethanol was used to resuspend the remaining

pellet, which was then centrifuged at 17,000 x g for 15 minutes. The remaining supernatant was discarded, and samples were air-dried until the remaining ethanol had evaporated. The remaining pellet was resuspended in 200µL of sterile water, and samples were stored at 4°C.

PCR Confirmation of *S. aureus* Strains

After DNA-extracting *S. aureus* strains, PCRs were used to confirm the presence of the desired plasmid and/or insert. PCR reactions were always set up with 1µL of DNA, 1µL of forward primer, 1µL of reverse primer, 9.6µL of sterile water, and 12.5 µL of polymerase enzyme. Thermocycling conditions vary based on the length of the amplified DNA, as well as the polymerase enzyme of choice.

ϕ11 Lysate Construction

All transductions were performed using ϕ11 lysates to transduce the desired clean background or mutant of choice. ϕ11 lysates were created by growing an overnight culture as previously described and adding 250µL of overnight into a sterile 15mL falcon tube. Subsequently, 5mL of TSB, 5mL of phage buffer, and 250µL of phage were added to the falcon tube. Lysates were incubated at 20°C overnight. They were then filter sterilized and stored at 4°C until use.

Transductions

All transductions were done as follows unless otherwise specified. 1mL of overnight culture from the desired background was added to a 15mL falcon tube. 12µL of 1M $CaCl_2$

was added, and subsequently 250µL of ϕ11 lysates of the desired insert was added. This mixture was then incubated in a 37°C water bath for 15 minutes. Subsequently, 2µL of 1% sodium citrate was added to the tube, mixed well, and centrifuged at 4150rpm for 10 minutes. The supernatant was discarded, and the pellet was then resuspended in 2mL of 0.5% sodium citrate solubilized in TSB. Tubes were then placed in the shaking incubator for 1 hour, and 100µL was plated onto agar with the appropriate selective antibiotic as described for *S. aureus.*

prsS Mutant Strain Construction

A *prsS* transposon mutant (NE166) was obtained from the Nebraska Transposon Mutant Library [43], and used to create a ϕ11 lysate to transduce USA300 HOU. This transposon mutant was confirmed using gene-specific primer OL6587 and transposon-specific primer OL1472. Subsequently, a Tetracycline marked USA300 LAC *spA::Tn* mutant was obtained from our lab stock (OL3141), and used to create a ϕ11 lysate to transduce USA300 HOU *prsS::Tn*, creating a double mutant. This double mutant was confirmed using the aforementioned primers for confirming *prsS::*Tn, as well as *spA* gene-specific primers OL5259 and OL5260. Primer sequences are provided (Table II).

prsS Complement Construction

A *prsS* complement was constructed using the previously described cloning protocol. PCR amplification of *prsS*, SAUSA300_0230, and its respective promoter was performed using primers OL6587 and OL6764 (Table II). The forward primer (OL6587) was created containing the SalI restriction site. The reverse primer (OL6764) was created with a 6xHis

tag embedded, and upon amplification this His tag was added to the C-terminus of *prsS*. Additionally, OL6764 was created containing the restriction site BamHI. This PCR product was cloned into pMK4, a gram-positive shuttle vector, through the transformation of DH5a. This clone was confirmed using pMK4-specific primers OL2393 and OL2394 (Table II), exhibiting an insert size corresponding to that of *prsS* and the surrounding pMK4 DNA (1,778 bp). *Staphylococcus aureus* RN4220 was electroporated with this clone, and was PCR confirmed again using pMK4-specific primers OL2393 and OL2394. A ϕ11 lysate of RN4220 pMK4::*prsS*+ 6xHis was used to transduce SAUSA300 HOU *prsS::Tn*, as well as SAUSA300 HOU *prsS::Tn spA::Tn*. The resulting complement strains were confirmed using pMK4-specific primers OL2393 and OL2394.

Alanine Substitution Library Creation

Using Agilent's provided primer design program, pairs of overlapping primers were made to create individual mutant alleles of each residue contained within the four protease motifs of PrsS (Table II). These primers were designed to create point mutations of each residue within these motifs into an alanine, apart from a native alanine residue at position 250 which was mutated to a serine; the valine at position 286 was ultimately mutated into a serine as well after multiple attempts at alanine substitution were unsuccessful (See Figure 4). The provided primer design program created primers that run opposite to each other on both the top and bottom strands of our template DNA, which for this study was our extracted plasmid pMK4::*prsS*+ 6xHis DNA. Each of these overlapping primers has the alanine codon embedded at the desired mutation site. These primers were run with our template DNA in the thermocycler with the following PCR reaction recipe provided in the mutagenesis kit: 38µL sterile water, 1µL of template plasmid DNA at a concentration

of 100ng/µL, 1.25µL of each primer containing the desired mutation site, 5µL of 10x buffer, 1µL of dNTP, 1.5µL of QuikSolution reagent, and 1µL of QuikChange Lightning Enzyme. After thermocycling, DpnI was used to digest the remaining template DNA. Then, provided *E. coli* XL-10 Gold Ultracompetent cells were used for transformation. This transformation was performed by thawing XL-10 competent cells on ice for 5 minutes and aliquoting 45µL of these competent cells into separate 1.5mL epi tubes per PCR reaction. 2µL of BME, provided in the kit, was added to these competent cells, and incubated at room temperature for 2 minutes. Following this, 2µL of DpnI digested PCR reaction was added, and mixed well. Then samples were incubated on ice for 30 minutes, where they were then heat shocked as described for traditional *E. coli* transformations and incubated on ice for an additional 2 minutes. 500µL of LB was added to each sample, which was then incubated in a 37°C water bath. Samples were then centrifuged at 12,000 x g for 5 minutes, and the supernatant was removed and discarded. The pellet was then resuspended in approximately 100µL of remaining LB, plated as previously described for *E. coli* with the appropriate antibiotic, and grown overnight. At this point, the steps previously described for traditional *E. coli* cloning follow suit. Colonies were PCR confirmed through colony PCR, re-streaked, grown overnight, plasmid extracted, and sent off for sequencing as described. Upon confirmation of sequencing, plasmids were transformed into RN4220, where they were again DNA extracted by *S. aureus* extraction methods, and PCR confirmed with pMK4 plasmid-specific primers (Table II). After PCR confirmation, phage lysates were created from RN4220 strains and were used to transduce USA300 HOU *spA::*Tn *prsS::*Tn as described. Once in our double mutant

background, plasmids containing our desired mutations were once again DNA extracted as described for *S. aureus*, and PCR confirmed using pMK4 plasmid-specific primers.

Alanine Stretch Library and Domain Deletion Creation

Using NEB's Base Changer primer design program, pairs of overlapping primers were made to create five amino acid stretch mutations within PrsS regions of unknown function. These regions included TMH 1, 2, and 8, as well as three separate regions in the C-terminal tail (see Figure 4). These alanine substitution primers were created by embedding five overlapping alanine codons on both the top and bottom strands in the desired mutation region (Table II). Additionally, we used NEB's Base Changer design program to create primers that produced a deletion mutant of PrsS missing the N-terminal extension (residues 2-107). These primers work by running one primer 5' to 3' on the top strand from amino acid residue 108, and the reverse primer running in the opposite direction from residue 1 (Table II). This results in primers synthesizing strands in opposite directions around the plasmid, until the strands meet, and the desired deletion region is not synthesized. These primers were run with our template DNA in the thermocycler with the following PCR reaction: 9µL sterile water, 1µL of template plasmid DNA at a concentration of 25ng/µL, 1.25µL of each primer containing the desired mutation site, and 12.5µL of Phusion DNA polymerase enzyme. Using the thermocycler settings as instructed in the kit, we ran the PCR reaction. Next, the KLD reaction was set up using: 1µL of PCR product, 5µL of 2X KLD reaction buffer, 1µL of 10X KLD enzyme mix, and 3µL of sterile water. All KLD reaction components were provided by NEB. This KLD reaction was incubated at room temperature for 2.5 hours. Next, we added 5µL of KLD

reaction product into 100µL of provided competent cells from the kit. The transformation at this point proceeds as previously described for *E. coli* transformations, with an ice incubation, heat shock, and 1-hour growth in LB. The resulting colonies were colony PCR confirmed, re-streaked, grown overnight, plasmid extracted, and sent off for sequencing as described. Upon confirmation of sequencing, plasmids were transformed into RN4220, where they were again DNA extracted by *S. aureus* extraction methods, and PCR confirmed with pMK4 plasmid-specific primers (Table II). After PCR confirmation, phage lysates were created from RN4220 strains and were used to transduce USA300 HOU *spA::*Tn *prsS::*Tn as described. Once in our double mutant background, plasmids containing our desired mutations were once again DNA extracted as described for *S. aureus*, and PCR confirmed using pMK4 plasmid-specific primers.

MMS Survival Assays

MMS survival assays were completed by growing overnight cultures of USA300 HOU *spA::Tn* pMK4 (wild type), USA300 HOU *spA::Tn prsS::Tn* pMK4 (mutant), and USA300 HOU *spA::Tn prsS::Tn* pMK4::*prsS*+ 6xHis (complement) strains alongside a maximum of five individual alanine-substituted mutant strains, all in biological triplicate. Cultures were synchronized and standardized as previously described, with standardized cultures grown for 2 hours. Each culture was then transferred to a 15mL falcon tube, centrifuged at 4150rpm for 10 minutes, and supernatants were discarded. The remaining cells were washed 3x with 1mL of PBS and centrifuged at 4150rpm for 5 minutes. After the final wash and centrifugation step, the remaining PBS was discarded, and cells were resuspended in 1mL of 50mM MMS solubilized in PBS. Treated cultures were incubated

shaking at 37°C and 250rpm for 15 minutes, after which PBS wash steps were repeated 3x. After the last wash, cells were resuspended in 1mL PBS and transferred directly to a 96-well plate. These cells were serially diluted in PBS to 10^{-7}. 8µL of each dilution, 10^{-3} through 10^{-7}, was plated on TSA Chloramphenicol in technical duplicates. Plates were incubated overnight, and individual colonies for each biological and technical replicate were counted the following day.

Data Analysis of MMS Screens

CFU/mL was calculated based on the colony count, the 8µL volume plated, and the dilution factor from which countable colonies were obtained. CFU/mL = ((Number of colonies x Dilution Factor) / (0.008mL)). Fold changes were calculated by dividing wild-type CFU/mL values by the CFU/mL values of the strain of interest. Fold changes were calculated for each technical duplicate, by dividing wild-type replicate 1 CFU/mL values by replicate 1 CFU/mL values of the strain of interest. All data was analyzed using a wild-type fold change value of -1. From performing these experiments in biological triplicate and plating them in technical duplicates, 6 separate fold change values were obtained from each strain per screen. All 6 of these fold change values were plotted as separate data points using Prism's graphing software. Statistical significance was determined by performing an unpaired t-test with Welch's correction between each mutant strain and the wild type, while not assuming equal standard deviations.

Protein Alignments

All protein alignments were completed using CLC Workbench, and all protein sequences were obtained from UniProt [46]. The UniProt protein sequences were cross-referenced with NCBI databases for accuracy. Additionally, the MEROPS peptidase database was used to search for additional members of the M82 family [45]; these members were cross-referenced through NCBI Blast as well.

Protein Fractionation for Western Blots

These methods are derived from an unpublished fractionation protocol by A. Weiss.

Liquid cultures of desired strains were grown overnight as previously described for *S. aureus.* Strains were then synchronized, standardized, and centrifuged at 4150rpm for 10 minutes. The supernatant was transferred to a 15mL falcon tube, where it was then precipitated with 10% TCA overnight at 4°C. This mixture was centrifuged at 4150rpm, and the resulting supernatant was used as the secreted fraction, stored at -80°C until use. The remaining pellets from our initial standardization were resuspended in 100µL of PBS, and 5µL of 2 mg/mL lysostaphin was added. This mixture was incubated for 30 minutes in a 37°C water bath, after which 2µL of DNAse was added, and incubation was repeated. This mixture was then centrifuged at 12,000 x g for 5 minutes, and the supernatant was collected and transferred to a separate epi tube comprising the soluble fraction. The remaining pellet was resuspended in solubilization buffer, which is water-solubilized and made with 4mL of 10% SDS, 2mL of 0.5M Tris at a pH of 7.4, and an overall 100mM concentration of DTT bringing the total volume to 10mL. This makes up the insoluble fraction. To all three fractions, 6x loading dye was added in a 5:1 ratio of dye to protein fraction. Loading dye is water-solubilized and made with 3.75mL 1M Tris-HCl at pH 6.8,

1g of SDS, 0.462g of DTT, 5mL of 100% glycerol, and 0.006g of bromophenol blue, and sterile water bringing the total volume to 10mL. Following the addition of loading dye, protein fractions were denatured by placing them in a heat block for 10 minutes at 95°C, and frozen at -20°C until use. Before western blotting, protein fractions were placed in the heat block again as described.

Western Blots

These methods are derived from an unpublished Western Blot protocol by A. Weiss.

Protein fractions were run alongside a protein ladder on 12% SDS page gels at 90V for roughly 2 hours or until the dye had reached the bottom of the gel. Before removing the gel, the blot construct was prepared in the semi-dry transfer tank. Blotting paper was soaked in a transfer buffer for 45 seconds before being placed in the semi-dry transfer tank. Then, the membrane was soaked in 100% methanol for 45 seconds, followed by an additional soak in a transfer buffer for 45 seconds. The membrane was then placed directly on top of the blotting paper on the semi-dry transfer machine. Next, the SDS page gel was removed and added to the top of the membrane. Finally, an additional piece of blotting paper soaked for 45 seconds in transfer buffer was placed on top of the gel. The semi-dry transfer tank was run at 20V for 45 minutes. When the semi-dry transfer was complete, the membrane was removed from the blotting paper and gel. The membrane was then placed into a rocking tray with 25mL of blocking buffer, which consists of 5% dry milk powder solubilized in a lab stock of TBST. This was incubated overnight at 4°C. The following day, the remaining blocking buffer was poured off the membrane and was replaced with 25mL of blocking buffer containing Invitrogen's 6x-His Tag Polyclonal anti-

Rabbit primary antibody at a 1:5000 ratio of antibody to blocking buffer. The membrane was left on a rocker in primary antibody at room temperature for 1 hour and then washed 3x for 10 minutes each in 25mL blocking buffer. Next, the LI-COR IRDye Goat anti-Rabbit IgG secondary antibody was added to 25mL of blocking buffer at a 1:20000 ratio of antibody to blocking buffer, added to the membrane, and incubated at room temperature for 1 hour. The membrane was washed 3x or 10 minutes in 25mL blocking buffer and developed on the LiCor imager directly as-is.

Western blots were performed as previously described on membrane, cytoplasmic, and secreted protein fractions of the USA300 HOU *spA::Tn prsS::Tn* double mutant, the USA300 HOU *spA::Tn prsS::Tn* pMK4::*prsS*+6xHis complementing strain, and the seven allelic variants previously determined to impact PrsS function in MMS (Table I). Each of these strains was confirmed in the membrane fraction at 42 kDa, the appropriate size of PrsS as determined by Expasy's molecular weight calculation tool, apart from the *prsS* mutant and the mutant allele of glutamic acid residue 216. Experiments were performed in biological triplicate.

Transcriptional Reporter Fusion Construction

The *prsS* promoter region was PCR amplified using primers OL7351/OL7352 and cloned into pXEN1 using restriction sites EcoRI and BamHI respectively. This construct was transformed into DH5a and confirmed via sequencing using pXEN1-specific primers OL5416 and OL5417, following the *E. coli* cloning and plasmid sequencing protocols previously described. Upon sequencing confirmation, this plasmid was electroporated

into RN4220 DNA was extracted, and constructs were PCR confirmed with OL5416/5417 following the protocols provided. A ϕ11 lysate of RN4220 pXEN1::P_{prsS}-*lux* was created and used to transduce over 100 JE2 transcription factor mutants as well as USA300 LAC [43].

Transducing Transcription Factor Mutants in 96-Well Format

These methods were adapted from Weiss et al., 2022 [44].

Glycerol stocks of 96-well plates 1 and 2, containing over 100 different transcription factor mutants [43], were used to inoculate 96-well plates containing fresh TSB and the appropriate antibiotics for each mutant at concentrations described for *S. aureus.* These freshly inoculated plates were wrapped in parafilm and grown overnight in 37°C shaking at 250rpm. The following day, 25µL of overnight culture contained in each well was transferred to new 96-well plates containing 175µL of fresh TSB with the appropriate antibiotic. Then, 20µL of ϕ11 lysate RN4220 pXEN1::P_{prsS}-*lux* and 2.4µL of 1M NaCl were added to each well of these new plates. These 96-well plates were then wrapped and incubated in the shaking incubator at 37°C and 250rpm for 30 minutes. After incubation, 6.7µL of sodium citrate was added to each well. Plates were again wrapped and centrifuged at 3500 rpm for 10 minutes. The supernatant was discarded, and the remaining pellet was resuspended in 200µL of TSB containing 0.5% sodium citrate. Following resuspension, plates were wrapped and incubated shaking at 37°C and 250rpm for 1 hour. 7µL from each well was plated onto TSA containing 0.5% citrate and the appropriate antibiotic selecting for pXEN1 (Chloramphenicol) and incubated overnight. The following day, single colonies from each plated culture were re-streaked for isolation

on TSA containing 0.5% citrate and Chloramphenicol. The following day, each construct was used to inoculate a single well in a new 96-well plate containing fresh TSB and Chloramphenicol. Plates were wrapped and incubated shaking at 37°C and 250rpm overnight. From these overnight cultures, glycerol stocks were made by adding 100µL of culture from each well into a new 96-well plate containing 100µL of 50% glycerol. Plates were stored at -80°C until use.

Luciferase Screen

These methods were adapted from Weiss et al., 2022 [44].

96-well plates containing glycerol stocks of transcription factor mutants with RN4220 pXEN1::P_{prsS}-*lux* were used to inoculate a 96-well plate containing fresh TSB and Chloramphenicol. The freshly inoculated plate was wrapped in parafilm and incubated shaking at 37°C and 250rpm overnight. The following day, 5µL of these overnight cultures were synchronized into a new 96-well plate containing 195µL of TSB and Chloramphenicol, otherwise following standard synchronization as previously described. Afterward, an OD_{600} reading of each well was taken using our plate reader. The appropriate amount of culture was used to standardize each strain into a new 96-well plate with 200µL TSB and Chloramphenicol per well. Following standardization, the plate was incubated in the plate reader for 18 hours, shaking intermittently. A luminescence reading was taken every 15 minutes throughout this time frame, and each time point per well was organized into Excel. Data was represented in relative light units (RLU). All luminescence experiments were performed in biological triplicate.

Luciferase screens were repeated on all constructs as previously described, with the addition of a final concentration of 1mM MMS in TSB and Chloramphenicol in the standardization step. All transcription factor mutants of interest from this screen were observed to impact *prsS* expression under standard conditions, apart from the *srrA* mutant, which was observed to impact *prsS* expression under MMS-induced conditions.

Data Analysis of Luciferase Screens

After acquiring luminescence reads in RLU for 71 different time points of 100 individual transcription factor mutants, we started by sorting this data into Prism. Using Prism's graphing software, each of these luminescence readings was graphed over time for each transcription factor mutant and the wild type. As each of these experiments was performed in biological triplicate, each graph contains error bars representing the standard error of the mean. Upon graphing these, we were also able to perform descriptive statistics of each graph in Prism, calculating the area under the curve of the transcription factor mutant and wild-type trend lines. Using these data analyses, we were able to identify potential activators and repressors of *prsS* activity based on the RLU emitted from our transcriptional reporter fusion in each of these transcription factor mutants.

Validations of Luciferase Data

To validate points of interest obtained from these luciferase screens, ϕ11 lysates of each transcription factor mutant of interest were transduced to a clean USA300 LAC background, following methods previously described. Each USA300 LAC transcription

factor transposon mutant was DNA extracted and PCR confirmed following our previous methods for *S. aureus*, using primers: OL7527/OL7528 for *purR::Tn,* OL7529/OL7530 for *glcT::Tn,* OL6840/OL6841 for *hrcA::Tn,* OL5365/OL5366 for *sarZ::Tn,* OL6053/OL6054 for *rsp::Tn,* OL238/OL3307 for *sigB::Tn,* and OL6039/OL6040 for *srrA::Tn.* Upon confirmation of these constructs, the ϕ11 lysate of RN4220 pXEN1::*PprsS-lux* was used once again to transduce these now-confirmed mutant strains in USA300 LAC. The insertion of our transcriptional reporter fusion plasmid was PCR confirmed using pXEN1-specific primers OL5416/OL5417 and the luciferase assay was repeated as previously described. All luciferase assays repeated with validated strains were performed in biological triplicate. The USA300 LAC *srrA::Tn* pXEN1::*PprsS-lux* construct was repeated in the presence of 1mM MMS in biological triplicate.

N-Terminomics Protein Fractionation

Overnight cultures of USA300 LAC wild type and USA300 LAC *prsS*::*Tn* were grown in biological triplicate in 50mL TSB flasks. The following day, these cultures were synchronized at a 1:100 dilution into new 50mL flasks and grown shaking for 3 hours as described. After synchronization, cultures were standardized to an OD_{600} of 0.05 and grown for 2 hours. Cultures were centrifuged at 4150rpm for 10 minutes, and the supernatant was discarded, as only soluble and insoluble fractions were needed for this experiment. Pellets were resuspended in PBS containing 100µg/mL of lysostaphin, 100U/mL of DNAse, 25U/mL of RNAse, and 2x protease inhibitor cocktail. Samples were then incubated at 37°C for 30 minutes. Following incubation, the remaining samples were lysed by bead-beating with 1MM glass beads and centrifuged at 17,000 x g for 10

minutes. The supernatant was removed comprising the soluble fraction, and the remaining pellet was used as the insoluble fraction. These fractions were resuspended in cell lysis buffer containing 5% SDS and 50mM TEAB at a pH of 8.5.

N-Terminomics

These methods are representative of work done in collaboration with Emilee Mustor.

A final concentration of 20mM DTT was added to our protein fractions, which were then placed in the heat block for 10 minutes at 95°C. Following this, samples were centrifuged at 17,000 x g for 10 minutes. A final concentration of 40mM iodoacetamide was then added to our samples, which were then incubated in the dark for 30 minutes at room temperature. A final concentration of 40mM DTT was then added. Samples were then incubated with 500mM HPCA and 500mM TEAB in the heat block for 10 minutes at 95°C. Samples were immediately incubated on ice for 5 minutes. Samples were then treated with 12% phosphoric acid, and a 1:7 ratio of sample to S-trap buffer (10% volume of TEAB at a pH of 7.5, and 90% volume of methanol). Proteins were run through the S-trap column, and centrifuged at 4000 x g for 1 minute, repeating this process 3x. Samples were then washed three times with 3mL S-trap buffer and centrifuged at 4000 x g for 1 minute. Trypsin/P (50mM TEAB at a pH of 8.1 containing 10µg of trypsin) was then added at a 1:100 ratio of enzyme to protein and then incubated for 18 hours at 37°C. Peptides were eluted following the S-trap protocol, where 50mM TEAB at a pH of 8.1, a 0.2% volume solution of formic acid, and 50% acetonitrile were each used for separate successive centrifugation steps. Samples were evaporated in a vacuum centrifuge to 1/3 of the final volume. Samples were then incubated with 100mM HEPES at a pH of 7.5,

containing 20mM SCBH and 20mM FDBA, for 1 hour at room temperature. 2 additional incubations were done using only 20mM SCBH and 20mM FDBA, for 1 hour and 16 hours respectively. A final concentration of 100mM Tris at a pH of 8.0 was then added. Samples were desalted using the Sep Pak C18 column protocol. Samples were then dried using a vacuum centrifuge. Samples were resuspended in 300µL of strong cation exchange buffer and vortexed and sonicated for 5 minutes each. Strong cation exchange columns were then equilibrated, and samples were added to the column and centrifuged for 5 minutes at 2000 x g. Samples were washed twice with 400µL of strong cation exchange buffer, and centrifuged for 5 minutes at 2000 x g each time. 200µL of strong cation exchange buffer B was added to the column and incubated for 1 minute before centrifuging for 5 minutes at 2000 x g. This step was repeated 1x. 1200µL of HPLC water was added, followed by 80µL of trifluoracetic acid. The Sep Pak C18 column protocol was followed once more, then peptides were dried using a vacuum centrifuge. Samples were stored at 4°C until mass spectrometry.

Table I. Strains and Plasmids

Strain or Plasmid	Genotype or Description	Reference or Source
Strains		
E. coli		
DH5a	Cloning strain	Salisbury et al., 1972
S. aureus		
RN4220	Restriction-deficient transformation recipient	Lab stock
NE166	USA300 JE2 *prsS::Tn*	Fey et al., 2013
NE286	USA300 JE2 *spA::Tn*	Fey et al., 2013
USA300	USA300 HOU MRSA isolate cured of pUSA300-HOU-MRSA	Highlander et al., 2007
	USA300 HOU *prsS::Tn,* pMK4::*prsS*$^{+}$ 6xHis	This study
OL3141	USA300 LAC *spA*::Tn	Lab Stock
	USA300 HOU *spA*::Tn, *prsS*::Tn	This study
	USA300 HOU *spA*::Tn, *prsS*::Tn, pMK4::*prsS*$^{+}$ 6xHis	This study
	USA300 HOU *spA*::Tn, *prsS*::Tn, pMK4::*prsS*^{E215A}	This study
	USA300 HOU *spA*::Tn, *prsS*::Tn, pMK4::*prsS*^{E216A}	This study
	USA300 HOU *spA*::Tn, *prsS*::Tn, pMK4::*prsS*^{T217A}	This study
	USA300 HOU *spA*::Tn, *prsS*::Tn, pMK4::*prsS*^{G218A}	This study
	USA300 HOU *spA*::Tn, *prsS*::Tn, pMK4::*prsS*^{K219A}	This study
	USA300 HOU *spA*::Tn, *prsS*::Tn, pMK4::*prsS*^{F249A}	This study
	USA300 HOU *spA*::Tn, *prsS*::Tn, pMK4::*prsS*^{A250S}	This study
	USA300 HOU *spA*::Tn, *prsS*::Tn, pMK4::*prsS*^{V251A}	This study
	USA300 HOU *spA*::Tn, *prsS*::Tn, pMK4::*prsS*^{F252A}	This study
	USA300 HOU *spA*::Tn, *prsS*::Tn, pMK4::*prsS*^{H284A}	This study
	USA300 HOU *spA*::Tn, *prsS*::Tn, pMK4::*prsS*^{L285A}	This study
	USA300 HOU *spA*::Tn, *prsS*::Tn, pMK4::*prsS*^{V286S}	This study

Table I. Continued

	USA300 HOU *spA*::Tn, *prsS*::Tn, pMK4::*prsS*^{W287A}	This study
	USA300 HOU *spA*::Tn, *prsS*::Tn, pMK4::*prsS*^{S288A}	This study
	USA300 HOU *spA*::Tn, *prsS*::Tn, pMK4::*prsS*^{H325A}	This study
	USA300 HOU *spA*::Tn, *prsS*::Tn, pMK4::*prsS*^{G326A}	This study
	USA300 HOU *spA*::Tn, *prsS*::Tn, pMK4::*prsS*^{I327A}	This study
	USA300 HOU *spA*::Tn, *prsS*::Tn, pMK4::*prsS*^{W328A}	This study
	USA300 HOU *spA*::Tn, *prsS*::Tn, pMK4::*prsS*^{D329A}	This study
	USA300 HOU *spA*::Tn, *prsS*::Tn, pMK4::*prsS*$^{Del.1-107}$	This study
	USA300 HOU *spA*::Tn, *prsS*::Tn, pMK4::*prsS*$^{Ala117-121}$	This study
	USA300 HOU *spA*::Tn, *prsS*::Tn, pMK4::*prsS*$^{Ala146-150}$	This study
	USA300 HOU *spA*::Tn, *prsS*::Tn, pMK4::*prsS*$^{Ala350-354}$	This study
	USA300 HOU *spA*::Tn, *prsS*::Tn, pMK4::*prsS*$^{Ala362-366}$	This study
	USA300 HOU *spA*::Tn, *prsS*::Tn, pMK4::*prsS*$^{Ala368-372}$	This study
	USA300 HOU *spA*::Tn, *prsS*::Tn, pMK4::*prsS*$^{Ala374-378}$	This study
	USA300 HOU pXEN1::*PprsS-lux*	This study
	USA300 JE2 *rsp::Tn* pXEN1::*PprsS-lux*	This study, Fey et al., 2013
	USA300 JE2 *sarA::Tn* pXEN1::*PprsS-lux*	This study, Fey et al., 2013
	USA300 JE2 *sarZ::Tn* pXEN1::*PprsS-lux*	This study, Fey et al., 2013
	USA300 JE2 *rpoF::Tn* pXEN1::*PprsS-lux*	This study, Fey et al., 2013
	USA300 JE2 *hrcA::Tn* pXEN1::*PprsS-lux*	This study, Fey et al., 2013

Table I. Continued

	USA300 JE2 *purR::Tn* pXEN1::*PprsS-lux*	This study, Fey et al., 2013
	USA300 JE2 *sarX::Tn* pXEN1::*PprsS-lux*	This study, Fey et al., 2013
	USA300 JE2 *glcT::Tn* pXEN1::*PprsS-lux*	This study, Fey et al., 2013
	USA300 JE2 *rot::Tn* pXEN1::*PprsS-lux*	This study, Fey et al., 2013
	USA300 LAC pXEN1::*PprsS-lux*	This study
	USA300 LAC *srrA::Tn* pXEN1::*PprsS-lux*	This study
	USA300 LAC *rsp::Tn* pXEN1::*PprsS-lux*	This study
	USA300 LAC *sarA::Tn* pXEN1::*PprsS-lux*	This study
	USA300 LAC *sarZ::Tn* pXEN1::*PprsS-lux*	This study
	USA300 LAC *rpoF::Tn* pXEN1::*PprsS-lux*	This study
	USA300 LAC *hrcA::Tn* pXEN1::*PprsS-lux*	This study
	USA300 LAC *purR::Tn* pXEN1::*PprsS-lux*	This study
	USA300 LAC *sarX::Tn* pXEN1::*PprsS-lux*	This study
	USA300 LAC *glcT::Tn* pXEN1::*PprsS-lux*	This study
	USA300 LAC *rot::Tn* pXEN1::*PprsS-lux*	This study
Plasmids		
pMK4		Sullivan et al., 1984
pXEN-1		Francis et al., 2000

Table II. Oligonucleotide Primers

Oligonucleotide Primers	Sequence	Source
OL6857 F *prsS*	atggtcgacgtcgtgccatgtgatttgtttcaag	This study
OL6764 R *prsS* 6xHis	catggatccttaatggtgatggtgatggtgttcgtctacttttttctgttgttc	This study
OL7351 F *prsS* promoter	atggaattcgaaatacaaagtgcccaatcgaacaaag	This study
OL7352 R *prsS* promoter	atgggatcccgatagattcattatgtatgtcggacgtc	This study
OL2393 F pMK4	tcgtatgttgtgtggaattg	Lab stock
OL2394 R pMK4	gtgctgcaaggcgattaag	Lab stock
OL5416 F pXEN-1	atcagagcagattgtactgag	Lab stock
OL5417 R pXEN-1	actcctcagagatgcgac	Lab stock
OL5259 F *spA*	tatgatgactttacaaatacatacaggggg	Lab stock
OL5262 R *spA*	gctcgtgcatttagatgattcttatcatt	Lab stock
OL1471 Transposon	tttatggtaccatttcattttcctgctttttc	Lab stock
OL1472 Transposon	aaactgatttttagtaaacagttgacgatattc	Lab stock
OL6747 F *prsS* E215A	taatgagtgcttttccagtttctgcaactaatcctactaaaaatgca	This study
OL6748 R *prsS* E215A	tgcatttttagtaggattagttgcagaaactggaaaagcactcatta	This study
OL6749 F *prsS* E216A	acaataatgagtgcttttccagttgcttcaactaatcctactaaaaatg	This study
OL6750 R *prsS* E216A	catttttagtaggattagttgaagcaactggaaaagcactcattattgt	This study
OL6751 F *prsS* K219A	gacgaaataaacaataatgagtgctgctccagtttcttcaactaatcctactaaa	This study
OL6752 R *prsS* K219A	tttagtaggattagttgaagaaactggagcagcactcattattgtttatttcgtc	This study
OL6753 F *prsS* F249A	gctgattcaaaaactgcggcccctgcaccaatagcagc	This study

Table II. Continued

OL6754 R *prsS* F249A	gctgctattggtgcaggggccgcagtttttgaatcagc	This study
OL6755 F *prsS* E253A	aaatataacctgctgatgcaaaaactgcgaaccctgcac	This study
OL6756 R *prsS* E253A	gtgcagggttcgcagtttttgcatcagcaggttatattt	This study
OL6757 F *prsS* H284A	aatcgctgaccaaactaaagcaccaccaatcgcagtccac	This study
OL6758 R *prsS* H284A	gtggactgcgattggtggtgctttagtttggtcagcgatt	This study
OL6759 F *prsS* H325A	gatgtatcccaaatgccagctaaaacaacggctgataaaaagaatattaaaaagc	This study
OL6760 R *prsS* H325A	gctttttaatattctttttatcagccgttgttttagctggcatttgggatacatc	This study
OL6761 F *prsS* D329A	gccaagtacagttaaagatgtagcccaaatgccatgtaaaacaac	This study
OL6762 R *prsS* D329A	gttgttttacatggcatttgggctacatctttaactgtacttggc	This study
OL6777 F *prsS* T217A	gatgcatttttagtaggattagttgaagaagctggaaaagcactcat	This study
OL6778 R *prsS* T217A	atgagtgcttttccagcttcttcaactaatcctactaaaaatgcatc	This study
OL6779 F *prsS* G218A	ttagtaggattagttgaagaaactgcaaaagcactcattattgtttatttc	This study
OL6780 R *prsS* G218A	gaaataaacaataatgagtgcttttgcagtttcttcaactaatcctactaa	This study
OL6799 F *prsS* A250S	ctattggtgcagggttctcagtttttgaatcagcag	This study
OL6800 R *prsS* A250S	ctgctgattcaaaaactgagaaccctgcaccaatag	This study
OL6801 F *prsS* V251A	ggtgcagggttcgcagcttttgaatcagcaggt	This study

Table II. Continued

OL6802 R *prsS* V251A	acctgctgattcaaaagctgcgaaccctgcacc	This study
OL6803 F *prsS* F252A	ctattggtgcagggttcgcagttgctgaatcagcaggttatatt	This study
OL6804 R *prsS* F252A	aatataacctgctgattcagcaactgcgaaccctgcaccaatag	This study
OL6805 F *prsS* L285A	tggactgcgattggtggtcatgcagtttggtcagcgattg	This study
OL6806 R *prsS* L285A	caatcgctgaccaaactgcatgaccaccaatcgcagtcca	This study
OL7195 F *prsS* W287A	ggactgcgattggtggtcatttagttgcgtcagcgattgttg	This study
OL7196 R *prsS* W287A	caacaatcgctgacgcaactaaatgaccaccaatcgcagtcc	This study
OL7197 F *prsS* S288A	gtggtcatttagtttgggcagcgattgttggtgct	This study
OL7198 R *prsS* S288A	agcaccaacaatcgctgcccaaactaaatgaccac	This study
OL7199 F *prsS* G326A	tatcagccgttgttttacatgccatttgggatacatctttaac	This study
OL7200 R *prsS* G326A	gttaaagatgtatcccaaatggcatgtaaaacaacggctgata	This study
OL7201 F *prsS* I327A	tatcagccgttgttttacatggcgcttgggatacatctttaactgtac	This study
OL7202 R *prsS* I327A	gtacagttaaagatgtatcccaagcgccatgtaaaacaacggctgata	This study
OL7203 F *prsS* W328A	tcagccgttgttttacatggcattgcggatacatctttaactgtac	This study
OL7204 R *prsS* W328A	gtacagttaaagatgtatccgcaatgccatgtaaaacaacggctga	This study
OL7274 F *prsS* V286S	gtggactgcgattggtggtcatttaagttggtcagcgattg	This study
OL7275 R *prsS* V286S	caatcgctgaccaacttaaatgaccaccaatcgcagtccac	This study

Table II. Continued

OL7607 F *prsS* N-terminal deletion (1-107)	aaaatgctcttttctcgagtattcatcg	This study
OL7532 R *prsS* N-terminal deletion	cccctcttcacctgtattag	This study
OL7577 F *prsS* TMH 1 Alanine Stretch (117-121)	tgctgctggattatgggtcatggcag	This study
OL7578 R *prsS* TMH 1 Alanine Stretch	gcagcagcgaaagcgatgaatactcgag	This study
OL7540 F *prsS* TMH 2 Alanine Stretch (146-150)	cgccgccggtttgttcttcttttatgaatc	This study
OL7541 R *prsS* TMH 2 Alanine Stretch	gcggcggctaaagcccctataaaaatg	This study
OL7544 F *prsS* TMH 8 Alanine Stretch (350-354)	cgccgccattttaatgggggcaggt	This study
OL7545 R *prsS* TMH 8 Alanine Stretch	gcggcggccacaataacgattaaaataaatattttcaac	This study
OL7579 F *prsS* C-terminal 1 Alanine Stretch (362-366)	tgctgctctgcagaaagaatttaaagaacaac	This study
OL7580 R *prsS* C-terminal 1 Alanine Stretch	gcagcagctaaacctgcccccattaaaatg	This study
OL7581 F *prsS* C-terminal 2 Alanine Stretch (368-372)	tgctgctgaacaacagaaaaaagtagac	This study
OL7582 R *prsS* C-terminal 2 Alanine Stretch	gcagcagccagtaaattcacttgttttaaac	This study
OL7583 F *prsS* C-terminal 3 Alanine Stretch (374-378)	tgctgctgacgaacaccatcaccatc	This study

Table II. Continued

OL7584 R *prsS* C-terminal 3 Alanine Stretch	gcagcagcttctttaaattctttctgcagtaaattc	This study
OL6053 F *rsp*	gttcgcaatgcataaaaacaagcg	Lab stock
OL6054 R *rsp*	ggtgtactgattaaatcggcaattaatgac	Lab stock
OL7527 F *purR*	gcggacctactgtgtatg	This study
OL7528 R *purR*	gcatgcgaatatggtccaagt	This study
OL7529 F *glcT*	ggataggcgtgtaatagaa	This study
OL7530 R *glcT*	cattcaattatagattcaccaccac	This study
OL6876 F *hrcA*	cacttgagataagtgagtgctaatg	Lab stock
OL6877 R *hrcA*	gtcctccaatactttctaatccatc	Lab stock
OL5365 F *sarZ*	cgatgaaatcagtacttgacaac	Lab stock
OL5366 R *sarZ*	acatatcgatgcatacttctgc	Lab stock
OL2896 F *sarX*	catgccatggctgaaaaatttaagataataatg	Lab stock
OL2897 R *sarX*	ccgctcgagaatatttaaaaattgttctacatc	Lab stock
OL3698 F *rot*	ccaatttagcctcattcggtttgatt	Lab stock
OL3699 R *rot*	tcatgctccattcatttgtgcc	Lab stock
OL3307 F *sigB (rpoF)*	atgcccgggtgccaagattgcagttagtg	Lab stock

Table II. Continued

OL238 R *sigB* (rpoF)	agctaggcatgcaatcctctactgatgtcg	Lab stock
OL6039 F *srrA*	tcaacacggtttgtttcttcacctttag	Lab stock
OL6040 R *srrA*	gaggtatgacctgtatgtcgaacg	Lab stock

CHAPTER THREE: RESULTS

Protein Sequence Alignment of the M82 Peptidases

An alignment of PrsW from *Bacillus subtilis*, PrsW from *Clostridium difficile*, and PrsS from *Staphylococcus aureus* protein sequences was created using CLC Workbench alignment software (Fig. 2). We see here that the conserved putative active sites of the M82 peptidases are maintained in this alignment, as all members contain the EEXXK, FXXXE, HXXXX, and HXXXD motifs [24]. PrsS shares 26 residues with *B. subtilis* PrsW that are not conserved in *C. difficile* PrsW. On the other hand, *B. subtilis* PrsW *and C. difficile* PrsW share 36 residues that are not conserved in PrsS, and *C. difficile* PrsW and PrsS share 35 residues that are not conserved in *B. subtilis* PrsW (Fig. 2).

Additionally, we can see that there are additional residues conserved across all members of the M82 peptidase family that have not been noted in previous literature. While they are not described as protease motifs, their level of conservation suggests that they may be important to structural conservation. These residues, relative to their position in *S. aureus* are, proline 136 and phenylalanine 152 contained in the second transmembrane helix (TMH). In the third TMH, we see a conserved phenylalanine at 172 and a glycine at 175. Interestingly, most of these uncharacterized residues are contained toward the C-terminal end of these proteins. In the fourth TMH, we see that phenylalanine 208, glycine

212, and isoleucine 222 are also conserved across all M82 peptidases. Notably, this glycine and isoleucine surround the first protease motif EEXXK (Fig. 2).

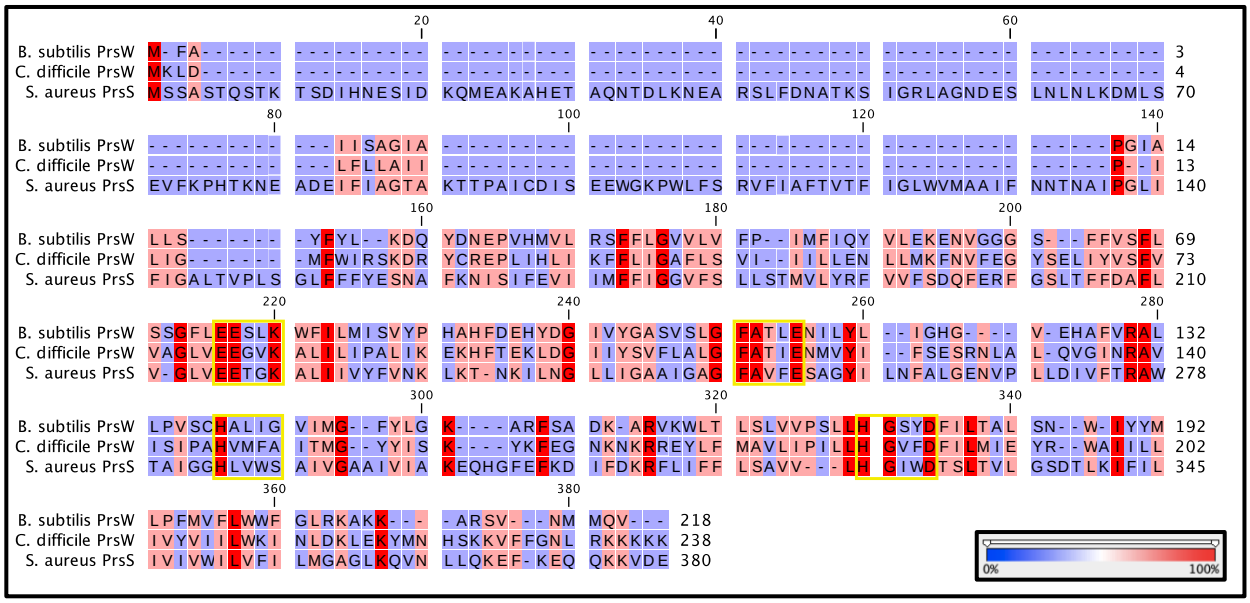

Figure 2. Protein alignment of M82 peptidases. A protein alignment of M82 peptidases: *Bacillus subtilis* PrsW*, Clostridium difficile* PrsW*, and Staphylococcus aureus* PrsS was created using CLC Workbench. Sequences were obtained from the UniProt database. The color of each residue indicates its percentage of conservation between all three peptidases, following the scale at the bottom. Blue indicates a residue contained in only one member, pink indicates a residue contained in two members, and red indicates 100% conservation across all three members of this peptidase family. Residues are numbered relative to their position in the alignment.

Entering the fifth TMH, we see the conservation of glycine 238, glycine 248 which immediately precedes protease motif FXXXE, and tyrosine 258 (Fig. 2). In the sixth TMH glycine 293 and lysine 300 are conserved. In TMH 7, arginine 313 and leucine 324 are also conserved. Notably, leucine 324 is present directly before protease motif HXXXD, and the second residue of this motif is a glycine for all three members (Fig. 2). In TMH 8, isoleucine 342 and leucine 352 are conserved across all M82 peptidases. Lastly, there are a few residues conserved across the three members of this family within the predicted

extra and intracellular loops, including arginine 276, alanine 277, phenylalanine 306, arginine 313, leucine 332, isoleucine 342, leucine 352 (Fig. 2). Additionally, there is conservation of one amino acid in the C-terminal tail – lysine 362. It's worth noting that conserved residues within the extracellular loops are only present in the last 20% or less of these proteins. An additional point of interest here is that there are no conserved residues within PrsS TMH 1 whatsoever, as this is still part of its lengthy N-terminal extension that is not present in other characterized M82 peptidases (Fig 2).

Discovering an M82 Homolog Through Protein Alignment

In searching through a phylogenetic tree from the MEROPS protein database [45], we discovered a fourth member of the M82 peptidases in *Lactobacillus brevis.* To validate this finding, we compared this uncharacterized protein with our alignment of the three known M82 peptidases seen in Figure 2. In this new alignment, we see that all conserved protease motifs are present in this *L. brevis* M82 homolog (Fig. 3). Additionally, this homolog contains 14 out of the 25 total non-protease motif conserved residues we found in Figure 2, most of which are contained within the transmembrane helices. The residues conserved across the known M82 peptidases and the *L. brevis* homolog, relative to their positions in PrsS, include a proline 136 in TMH 2. In TMH 3, phenylalanine 172 and glycine 175 are still conserved. Additionally, we see that *L. brevis'* homolog also contains the glycine at 212 in TMH 4, glycine 238, glycine 248, and tyrosine 258 in TMH 5. Final conserved residues within the transmembrane domains include glycine 293 and lysine 300 in TMH 6, as well as arginine 313 and leucine 324 in TMH 7. This M82 peptidase in *L. brevis* also contains four conserved residues within the extra- and intra-cellular loops

of the M82 peptidases, including arginine 276, phenylalanine 306, and leucine 332 (Fig. 3). Additionally, there is conservation of one C-terminal tail amino acid – lysine 362.

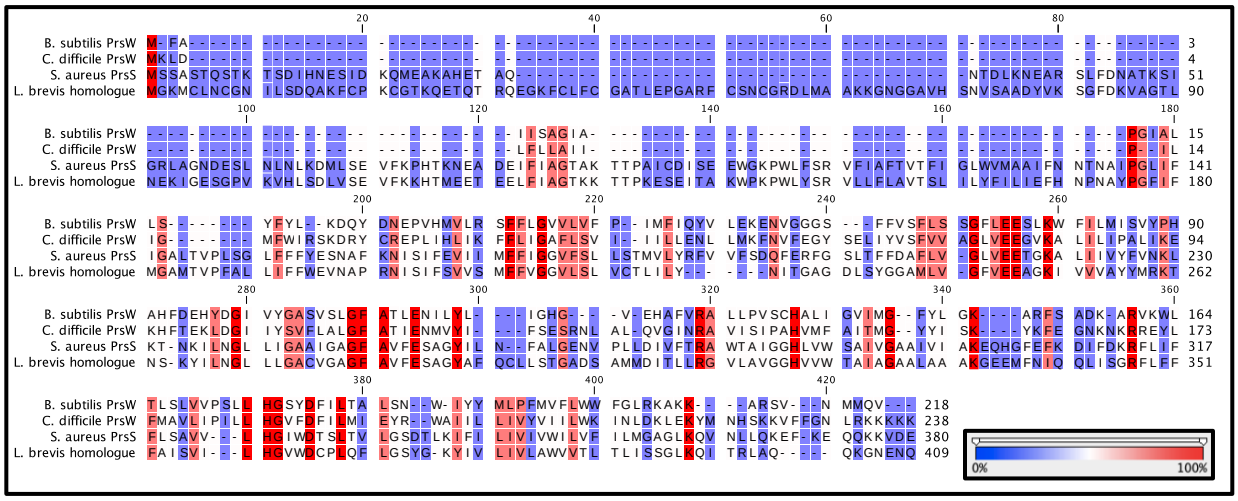

Figure 3. Discovery of an M82 homolog through protein alignment. A protein alignment of the three M82 peptidases: *Bacillus subtilis* PrsW*, Clostridium difficile* PrsW*, and Staphylococcus aureus* PrsS *was* compared to a homolog found in *Lactobacillus brevis* using CLC Workbench. Sequences were obtained from the UniProt database. The color of each residue indicates its percentage of conservation between all three peptidases, following the scale at the bottom. Blue indicates a residue contained in only one member, white indicates a residue contained in two members, pink indicates a residue contained in three members, and red indicates 100% conservation across all four proteins in this alignment.

This M82 peptidase in *L. brevis* shares an interesting structural similarity with *S. aureus* PrsS as well, as they both contain lengthy N-terminal tails that are not found in either of the PrsW proteins. However, the N-terminal tails of PrsS and this *L. brevis* homolog show virtually no residue conservation. Similarly, these *L. brevis* and *S. aureus* M82 peptidases each contain 8 transmembrane domains, whereas the PrsWs only contain 7. These results tell us that while the conserved transmembrane domains of *S. aureus* PrsS and *L. brevis* M82 peptidase are found in TMHs 4-7, these conserved transmembrane domains of the PrsWs are found in TMHs 3-6.

PrsS Predicted Structure and Mutagenesis Library

Using Protter's protein visualization tool [51], we generated a predicted topology plot of PrsS (Fig. 4). This visual representation shows us an estimate of where the N-terminal extension and C-terminal tail of PrsS are located, where the intra- and extra-cellular loops are found, and where each of the eight transmembrane helices begins and ends. Using this tool as a visual aid, we mapped out the domains, protease motifs, and regions of unknown function contained within PrsS to use as a guide for future experiments. As PrsS has been observed to assist *S. aureus* in responding to DNA damage through its proteolytic activity [23], we chose to create mutant alleles of this protein to evaluate the functional importance of specific structures in the cell's ability to respond to DNA-damaging agents. This topology map demonstrates each of the individual alanine substitutions, alanine stretch mutations, and domain deletions created and evaluated for their ability to complement the PrsS ability to assist in cellular stress response.

As seen in Figures 2 and 3, each of the protease motifs is contained in TMHs 4-7 of PrsS. The highlighted portions in Figure 4, corresponding to individual mutations in the key, indicate the singular alanine substitution mutants that were created for each residue contained within these predicted protease motifs of TMHs 4-7. Additionally, the highlighted portions in TMHs 1, 2, and 8, as well as the three sections of the C-terminal tail, indicate alanine stretch mutants that were created 5 amino acids at a time. Finally, the N-terminal section highlighted is representative of a deletion mutant made, where we removed amino acids 2-107 of PrsS.

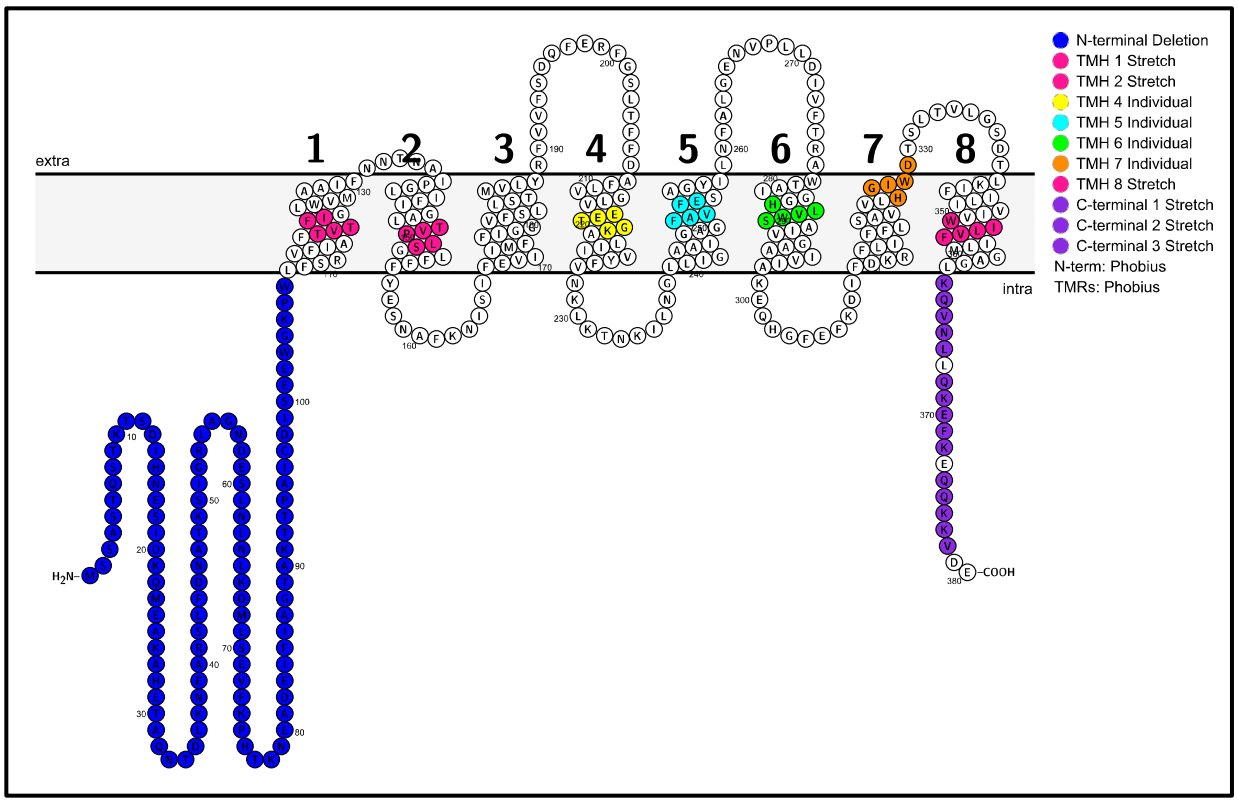

Figure 4. Visualization of *prsS* mutagenesis library. A predicted structure of PrsS was generated using Protter. Each strain from our mutagenesis library can be visualized here, following the color-coded key at the top. The grey section is representative of the membrane, and the black numbers indicate transmembrane helices 1-8. “Stretch” is used to describe a stretch of 5 amino acids converted to alanine residues at once. “Individual” is used to describe 5 amino acids that were individually converted to alanine residues, each creating a separate strain.

While the alignments in Figures 2 and 3 help us visualize the conserved residues and protease motifs across M82 peptidases, this Protter rendition of PrsS in Figure 4 helps us identify structural domains and their limits within this *S. aureus* protease [51]. In creating this predicted topology map, we can observe some inconsistencies when comparing the structure of PrsS to the PrsWs. These differences include the number of total transmembrane helices in PrsS, exactly where each protease motif is located within these TMHs, the locations of the extra- and intra-cellular loops, and the length of both the N-terminal extension and the C-terminal tail. This visual aid of our PrsS mutagenesis library shows where and how we’ve altered individual residues within the protease motifs, as

well as unique PrsS regions of unknown function, allowing us to evaluate which structural components of this M82 peptidase are necessary for proteolytic activity and thus, circumventing DNA-damage stress in *S. aureus*.

Mutations of Three Key Residues in TMD 4 Impact PrsS Function

Each individual residue from the first protease motif, contained within transmembrane domain 4, was substituted to alanine. Each of these mutant alleles was tested for their ability to complement the MMS sensitivity of the mutant, alongside the wild-type and complement strains, allowing us to see which of these substitutions impact PrsS function. The mutant shows a decreased ability to survive in MMS, with a resulting CFU/mL of -1.89x fold of the wild type (Fig. 5). The glutamic acid alanine substitutions at positions 215 and 216 show a similar survival phenotype to the mutant, with CFU/mL values at -1.74x and -1.65x fold change from the wild type respectively (Fig. 5). Alanine substitution K219 also displays decreased survival after MMS exposure, resulting in a -1.66x fold change from the wild type (Fig. 5). The complement, as well as residues 217 and 218, did not show a significant fold change reduction from the wild type (Fig. 5). As we did not see reduced survivability in three of these alanine substitutions, we can conclude that as individual residues, they are not necessary for PrsS to elicit a response to DNA-damage. As the first two residues of this protease motif have been evaluated for functional necessity before [23], and here we present confirmation of previous work from the literature. However, the lysine residue at position 219 had not previously been assessed for protein function. This result is a new development across all M82 peptidase research, as K219 is conserved through each member of this family.

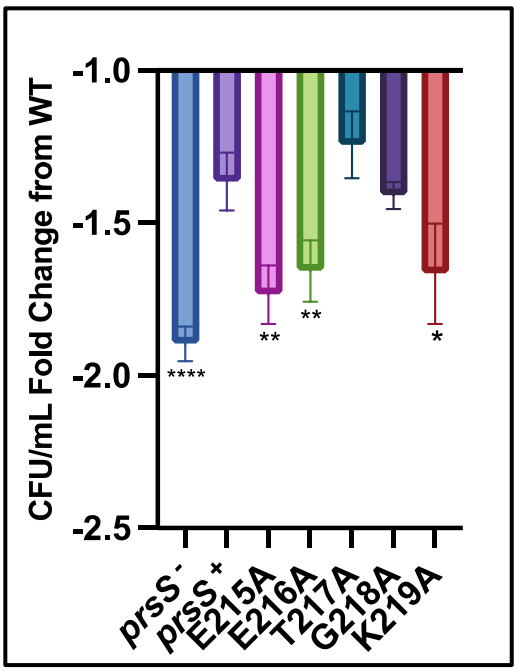

Figure 5. Three residues in TMD 4 are necessary for PrsS function. Individual alanine substitution mutants were treated with 50mM MMS for 15 minutes alongside the wild type, mutant, and complement strains. Cultures were serial diluted, plated, and grown for 16-18h. CFU/mL was calculated for each strain and is shown as fold-change from the wild type. Each experiment was completed in biological triplicate and plated in technical duplicates. Significance was determined using an unpaired t-test with Welch's correction (*, p< 0.05; **, p<0.01; ****, p<0.0001), and error bars are shown representing ±SEM.

Mutation of One Key Residue in TMD 5 Impacts PrsS Function

Continuing our MMS survival screens, each residue from the second protease motif, present in TMD 5, was individually substituted to alanine apart from the native alanine at position 250 being mutated to serine. These mutant alleles were tested for their ability to complement the MMS sensitivity of the mutant, alongside the wild type and complement strains, allowing us to evaluate reduced survivability. We found one residue in TMD 5 that mimics the mutant's response to MMS, proving to be necessary for PrsS to facilitate a response to DNA damage. The glutamic acid residue at position 253 showed reduced survival upon MMS exposure, with a CFU/mL value of -1.51x fold change from the wild type. The complement, as well as substituted residues 249, 250, 251, and 252, did not

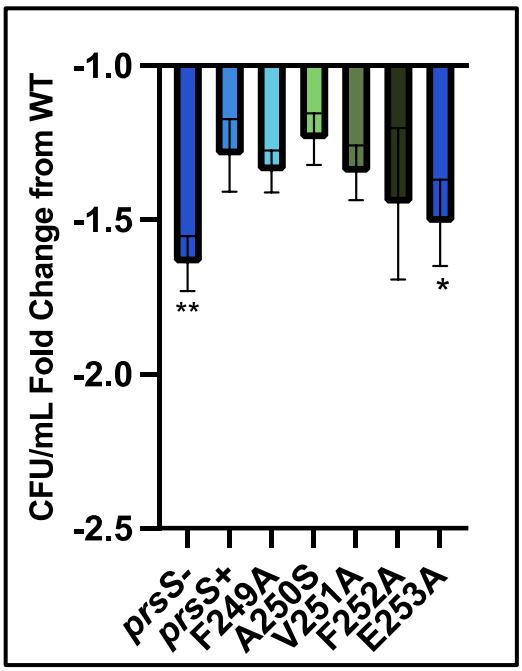

Figure 6. Two residues in TMD 5 are necessary for PrsS function. Individual alanine substitution mutants were treated with 50mM MMS for 15 minutes alongside the wild type, mutant, and complement strains. Cultures were serial diluted, plated, and grown for 16-18h. CFU/mL was calculated for each strain and is shown as fold-change from the wild type. Each experiment was completed in biological triplicate and plated in technical duplicates. Significance was determined using an unpaired t-test with Welch's correction (*, $p < 0.05$; **, $p<0.01$), and error bars are shown representing ±SEM.

show a significantly reduced fold change in CFU/mL compared to the wild type. The glutamic acid residue 253 is both contained within a protease motif and conserved across all M82 peptidases. Interestingly, the phenylalanine at position 249 also falls within a protease motif. While this residue is also conserved across all M82 peptidases, it does not appear to be individually necessary for PrsS function.

Mutation of One Key Residue in TMD 6 Impacts PrsS Function

All residues from the third protease motif in TMD 6 were mutated to alanine, apart from the valine at position 286. This valine was mutated to a serine, as attempts to create an alanine substitution at this residue were repeatedly unsuccessful. Each of these

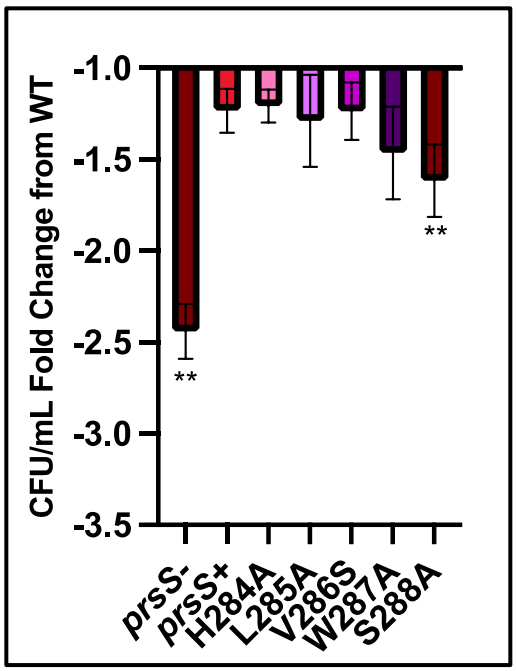

Figure 7. One residue in TMD 6 is necessary for PrsS function. Individual alanine substitution mutants were treated with 50mM MMS for 15 minutes alongside the wild type, mutant, and complement strains. Cultures were serial diluted, plated, and grown for 16-18h. CFU/mL was calculated for each strain and is shown as fold-change from the wild type. Each experiment was completed in biological triplicate and plated in technical duplicates. Significance was determined using an unpaired t-test with Welch's correction (**, $p<0.01$), and error bars are shown representing ±SEM.

mutant alleles were treated with MMS to evaluate their ability to complement mutant levels of survival alongside the wild-type and complement strains. The serine residue at position 288 displayed a partially reduced capacity for survival, although not to the level of the mutant. The CFU/mL values obtained from this S288A alanine substitution post-MMS treatment displayed a -1.62x fold change from the wild type (Fig. 7). Alternatively, the complement and residues 284, 285, 286, and 287 did not show a significant loss of function in their respective fold change values from the wild type. Contrary to Figure 4 where the mutant alleles of all three residues conserved across the M82 peptidases exhibited reduced survival, here we see that conserved histidine 284 does not appear to

be necessary for PrsS to circumvent DNA damage. Alternatively, the mutant allele of the valine at position 288 partially complements the mutant post-MMS treatment, however, it is not a conserved residue across the M82 peptidases. This would suggest that this residue is only partially necessary for the PrsS response to DNA-damaging stress and that perhaps it contributes structural stability to PrsS as opposed to proteolytic activity.

Mutations of Two Key Residues in TMD 7 Impact PrsS Function

In this final MMS screen, we created allelic variants of all residues in protease motif four, contained within TMD 7, by substituting them with alanine residues. After MMS exposure, CFU/mL was calculated and evaluated for statistical significance, using -1.5x fold change as the cutoff for determining reduced survivability. Residue mutations that result in reduced survival post-MMS treatment include both a tryptophan at position 328 and an aspartic acid at position 329. This experiment was particularly interesting, as we see a -1.95x fold change from the wild type upon alanine substituting tryptophan (W328A), but a -3.28x fold change from the wild type upon substitution of aspartic acid (D329A) (Fig. 8). While the substitution of residue W328 seems to mirror the reduced response to DNA-damage seen in the *prsS* mutant, altering D329 seems to negatively impact the cells' survival in MMS even more so than the *prsS* mutant.

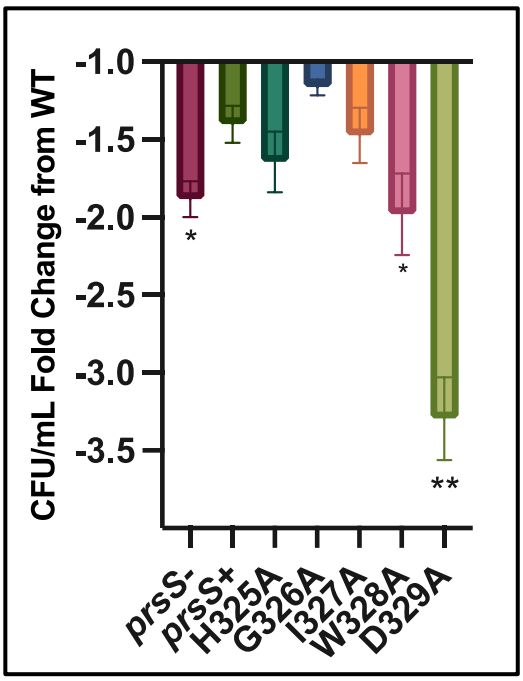

Figure 8. Two residues in TMD 7 are necessary for PrsS function. Individual alanine substitution mutants were treated with 50mM MMS for 15 minutes alongside the wild type, mutant, and complement strains. Cultures were serial diluted, plated, and grown for 16-18h. CFU/mL was calculated for each strain and is shown as fold-change from the wild type. Each experiment was completed in biological triplicate and plated in technical duplicates. Significance was determined using an unpaired t-test with Welch's correction (*, $p< 0.05$; **, $p<0.01$), and error bars are shown representing ±SEM.

As for residues 325, 326, and 327, we do not see a significantly reduced ability to survive upon exposing the allelic variant substitutions of these residues to MMS (Fig. 8). Interestingly, upon mutation of the histidine at position 325, we observed a reduced survivability beyond the -1.5x fold change cutoff, however, the data was not statistically significant at a p-value of 0.08. As this is a conserved residue contained within a protease motif, further studies may be needed to evaluate its importance in both PrsS and other M82 peptidases. Additionally, while the G326A substitution did not result in reduced survivability in MMS, this residue is conserved across all M82 peptidases including the most recently found homolog in *L. brevis*; and is contained within a protease motif. The

conservation of this residue across the M82 peptidases may suggest that it contributes either structural importance or functional importance to different external stressors.

MMS Survival in Unique PrsS Regions

In Figure 9, we created multiple-allelic variants consisting of five consecutive amino acids, each in various structural regions of PrsS with no prior known function. These variants were created to evaluate the importance of transmembrane domains 1, 2, and 8, as well as three separate sections of the C-terminal tail. Additionally, we created an N-terminal deletion variant of PrsS as well, where we removed amino acids 2-107. Each of these allelic variants can be visualized in Figure 3. These mutants were screened for their ability to complement the reduced MMS survival of the *prsS* mutant by the same process used in Figures 5-8.

Concerning mutations in TMH 1, TMH 2, and TMH 8, the final two sections of the C-terminal tail, and our N-terminal deletion, we saw no change in survival following MMS treatment, as compared to the parent and complemented strain. This would indicate that neither TMH 1, TMH 2, TMH 8, the final two sections of the C-terminal tail, nor the lengthy N-terminal extension are necessary for PrsS function (Fig. 9). As none of these regions are highly conserved with the other members of the M82 peptidase family, it would suggest that perhaps they don't contain vital functional components of this protein. Instead, they may contribute to structural support or folding integrity.

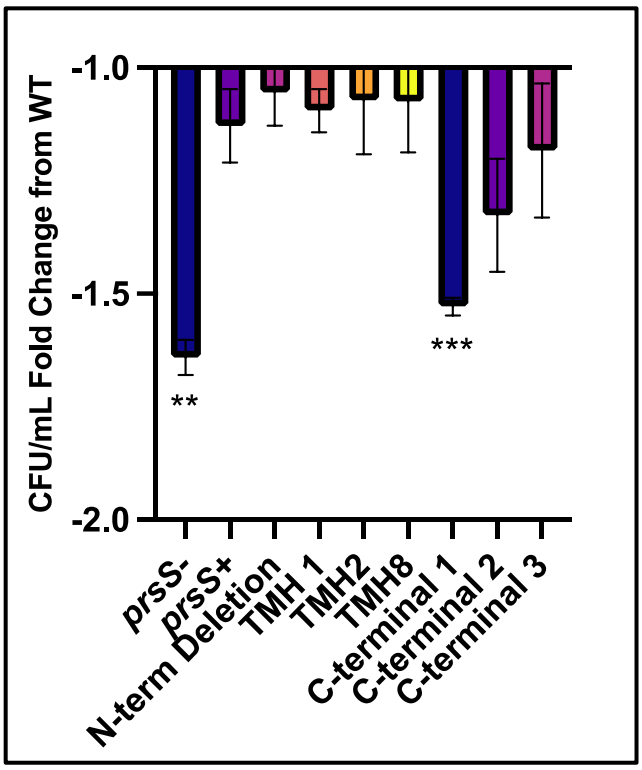

Figure 9. The first 5 amino acids of the CTT are necessary for PrsS function. Alanine stretch mutants, as well as the N-terminal deletion mutant, were treated with 50mM MMS for 15 minutes alongside the wild type, mutant, and complement strains. Cultures were serial diluted, plated, and grown for 16-18h. CFU/mL was calculated for each strain and is shown as fold-change from the wild type. Each experiment was completed in biological triplicate and plated in technical duplicates. Significance was determined using an unpaired t-test with Welch's correction (**, $p<0.01$; ***, $p<0.001$), and error bars are shown representing ±SEM.

However, the alanine stretch mutant created in which we substituted the first five amino acids of the PrsS C-terminal tail did exhibit significantly reduced survival, with a fold change of -1.62x from the wild type (Fig. 9). This indicates that at least one residue contained within the first 5 amino acids of the C-terminal tail is necessary for function or structural integrity. While this amino acid stretch immediately follows transmembrane domain 8, it's possible that this stretch mutation could be affecting this transmembrane helix structurally as well. From our alignments and structural prediction of PrsS, we can see that there is one conserved residue across all members of the M82 peptidase family,

including the homolog in *L. brevis,* found in the C-terminal tail of PrsS. That residue, a lysine at position 362, is the first residue of 5 contained within the C-terminal alanine stretch demonstrating reduced survivability in Figure. 9.

Membrane Localization of PrsS and Alanine-Substituted Mutants

Western blots of protein fractions extracted from the *prsS* mutant and complement strains were performed alongside alanine substituted mutants of the seven residues we found to be necessary for PrsS function in Figures 5-8. Here, we see that the PrsS is membrane-associated, like other members of the M82 peptidases, and consistently appears in the membrane fraction as shown in Figure 10 at the appropriate size of 42 kDa. We see that alanine substituting the majority of these residues, specifically glutamic acid 215, lysine 219, glutamic acid 253, serine 288, tryptophan 328, and aspartic acid 329, still result in stable PrsS protein production as these proteins consistently show up in the membrane fraction around 42 kDa alongside the *prsS* complement (Fig. 10). However, upon alanine substitution of the glutamic acid at 216, the subsequent protein produced is no longer present across any of our three entirely separately conducted trials. Instead, this substitution results in a phenotype resembling the mutant in its absence from not only the membrane, but all three protein fractions blotted (Fig. 10). This would suggest that the alanine substitution of glutamic acid 216 results in an unstable PrsS protein production, leading to its subsequent degradation and therefore absence on these western blots. As this residue has shown to be necessary for PrsS function, these western blots may give us some insight into why that is. It's possible that the substitution of this conserved residue

contained within the first protease motif completely derails the proper folding of this M82 peptidase.

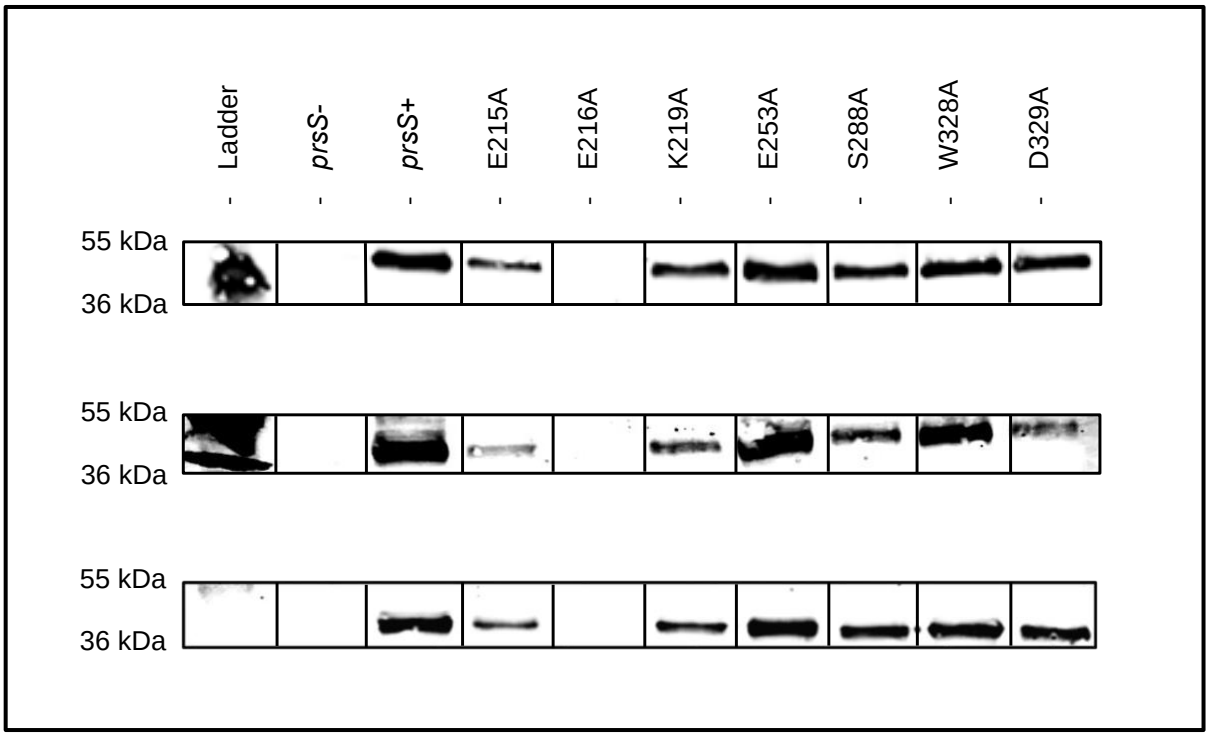

Figure 10. Glutamic acid residue 216 is required for PrsS protein stability. A western blot was performed on the secreted, cytoplasmic, and membrane protein fractions from the *prsS* mutant and complement strains, as well as the seven individual mutant alleles found to impact PrsS function (Fig. 5-8). Rabbit anti-His tag primary antibody was used, followed by goat anti-rabbit IgG-HRP conjugate secondary antibody. We see PrsS expression in the membrane fraction shown above at approximately 42 kDa. PrsS is predicted to be 42.18 kDa by Expasy's molecular weight calculation tool.

***prsS* Expression is Influenced by Major Transcriptional Regulators**

In efforts to understand how *prsS* expression is regulated in *S. aureus,* we performed a mass screen in over 100 different transcription factor (TF) mutants using the transcription reporter fusion P_{prsS}-*lux,* which emits light upon transcriptional activation [43]. This screen allows us to visualize which major *S. aureus* transcriptional regulators are both activating and repressing *prsS* expression.

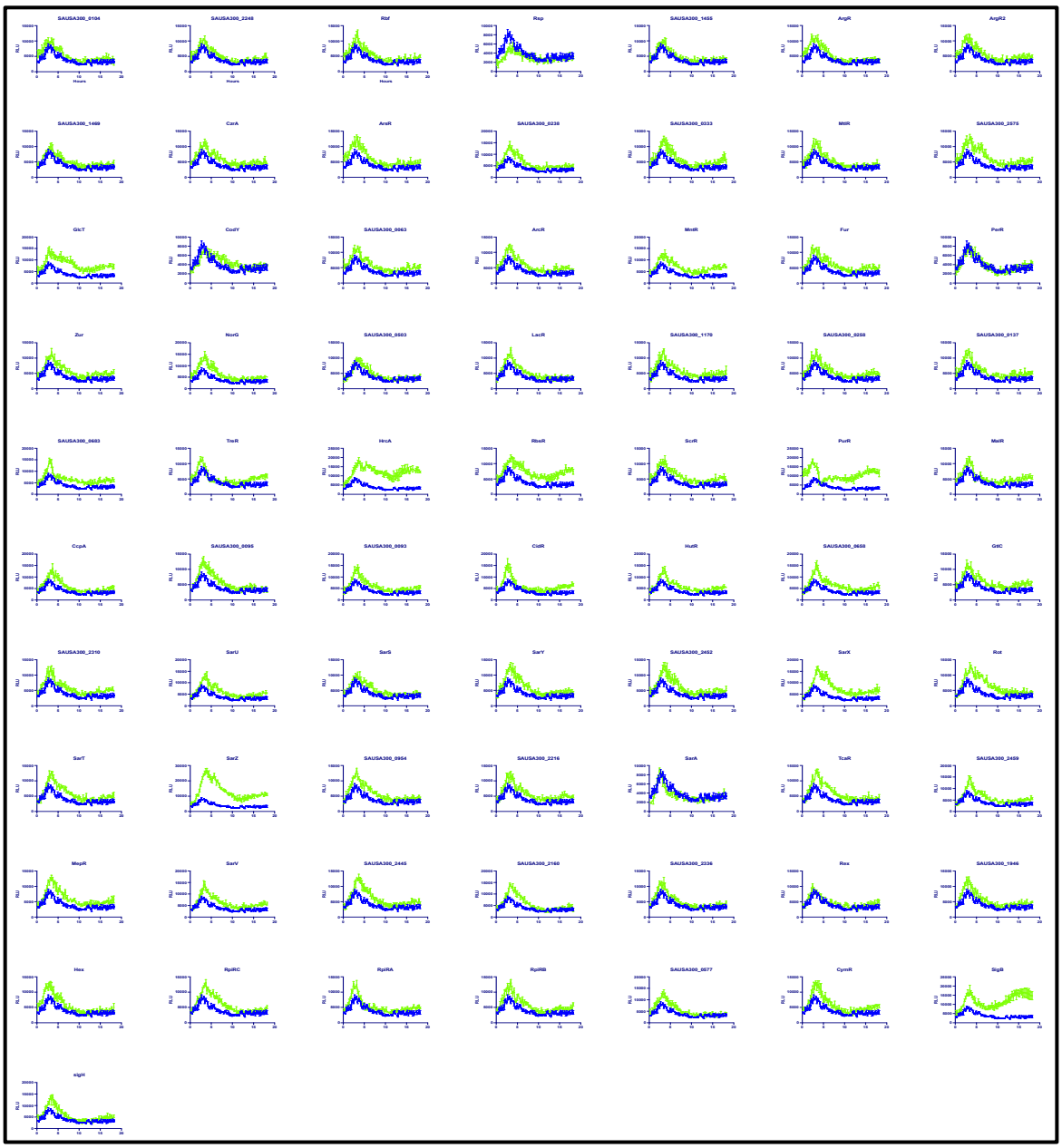

Figure 11. *prsS* promoter activity in transcription factor mutants. The pXEN1:P$_{prsS}$-*lux* plasmid was transduced into JE2 transcription factor mutants from Plate 1. Luminescence was recorded in relative light units (RLU) over 18 hours. The data shown represents *prsS* expression in each transcription factor mutant (green) compared to the wild type (blue). Each experiment was completed in biological triplicate, and error bars are shown representing ±SEM.

Figure 11 displays graphs of relative light units (RLU) expressed by our transcriptional reporter fusion, every 15 minutes over 18 hours, in individual JE2 TF mutant strains and the wild type. To sort through these large data sets, we've taken a few different

approaches to narrowing down transcription factors that influence *prsS* expression. In graphing each RLU value associated with each time point depicted in Figure 11, we were able to calculate the area under the curve (AUC) values of each TF mutant alongside the wild-type AUC values. Performing these analyses and using Figure 11 as a visual aid helps clarify which of the mutants have differences in *prsS* expression when compared to the wild type. In Figure 11, we see that the graph containing the *rsp* mutant is the only one in which the wild-type values of RLU, correlating to *prsS* expression, surpass the TF mutant values. This suggests that in the presence of Rsp, *prsS* expression is activated. Alternatively, in graphs of the *sarZ*, *hrcA, sigB, purR,* and *glcT* mutants *prsS* expression appears to be activated, indicating that these transcription factors repress *prsS* activity. Graphing this data individually is a beneficial step for conceptualizing the AUC data shown in Figures 12 and 13, and additionally provides visual context for each transcription factor's influence on *prsS* expression in varying stages of growth.

Area Under the Curve Analysis of *prsS* Regulators

In Figure 12, we further quantified our data sets to numerically evaluate the transcription factors that had the greatest effect on *prsS* promoter expression. Using a +1.5x fold cutoff for pinpointing repressors of *prsS,* we observed the greatest area under the curve of values of RLU/Time in the *sarZ, hrcA, sigB, purR,* and *glcT* mutant strains. These high area under the curve values tell us that in the absence of these transcription factor mutants, the *prsS* expression is activated. From this, we can infer that these transcriptional regulators are each repressing *prsS* activity in the wild type.

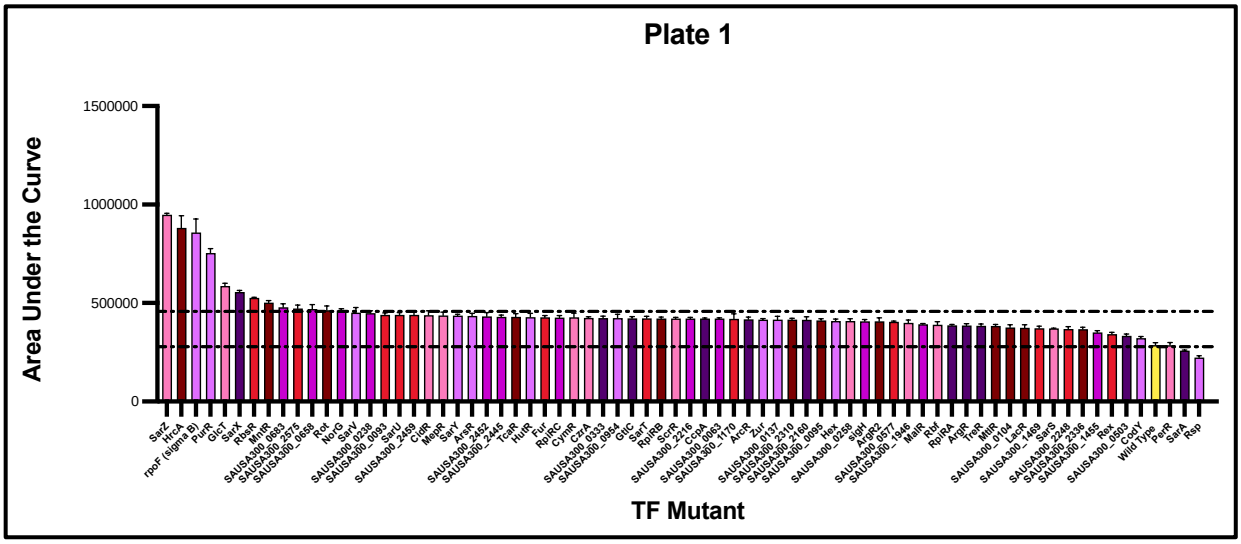

Figure 12. Using AUC to identify transcriptional regulators of *prsS* in plate 1. The pXEN1:P$_{prsS}$-*lux* plasmid was transduced into USA300 JE2 transcription factor mutant strains, and the luminescence of each construct was measured in relative light units (RLU) over 18 hours. The data shown represents the area under the curve analysis for each transcription factor mutant and the wild type. The dotted lines represent a 1- and 1.5-fold difference in total AUC from the wild type. Each experiment was completed in biological triplicate, and error bars are shown representing ±SEM.

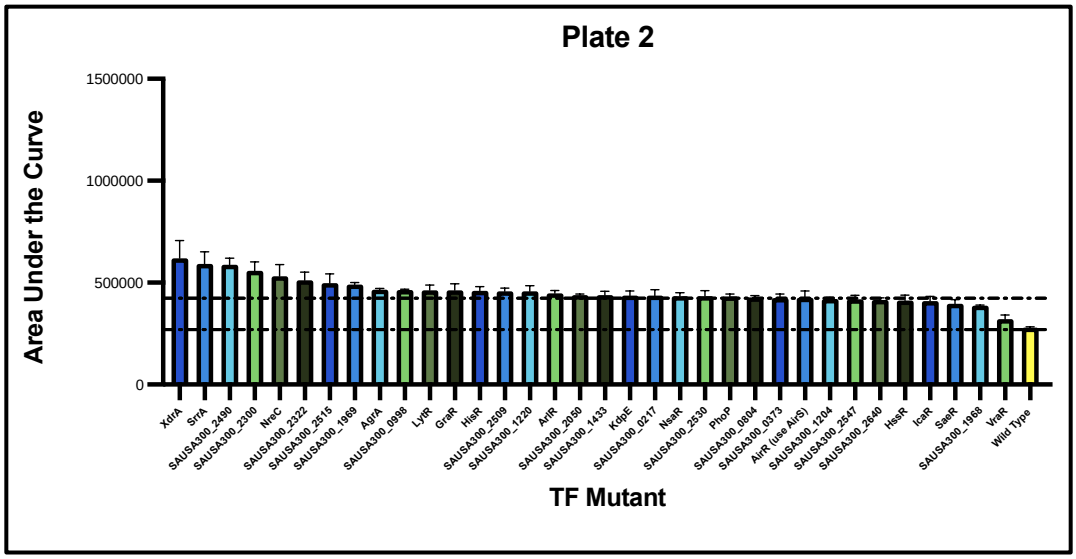

Figure 13. Using AUC to identify transcriptional regulators of *prsS* in plate 2. The pXEN1:P$_{prsS}$-*lux* plasmid was transduced into USA300 JE2 transcription factor mutant strains, and the luminescence of each construct was measured in relative light units (RLU) over 18 hours. The data shown represents the area under the curve analysis for each transcription factor mutant and the wild type. The dotted lines represent a 1- and 1.5-fold difference in total AUC from the wild type. Each experiment was completed in biological triplicate, and error bars are shown representing ±SEM.

On the low ends of our area under the curve data, we see that the only value considerably lower than the wild type is observed in the *rsp* mutant. This tells us that in the absence of Rsp, *prsS* expression is repressed, suggesting that this transcription factor is a potential activator of *prsS.* In Figure 13, we see that there are no transcriptional regulators impacting *prsS* expression in Plate 2 to the degree of those observed in Plate 1.

Validation of *prsS* Repressors

As each of the strains used to complete our screenings from Figures 11-13 were USA300 JE2 mutants obtained from the Nebraska Transposon Mutant Library, we chose to confirm these strains in one of our lab wild-type strains, USA300 LAC. By transducing these transcription factor mutants into a clean LAC background, we confirmed that these effects on *prsS* expression are not solely found in the USA300 JE2 background. We observed little difference in the expression patterns of *prsS* in these validated LAC transcription factor mutants from our original screening data. Each predicted repressor from our previous screens in Figure 12 was observed to repress *prsS* activity in a clean LAC background (Fig. 14). As shown in Figure 14, in the mutants of *sarZ, hrcA,* and *sarX, prsS* transcription is activated at the start of exponential phase (Fig. 14A, 14D, 14F). However, we see some differences in the timing of *prsS* activation in the *purR, sigB,* and *glcT* mutants. In the *purR* mutant, *prsS* promoter activity is upregulated at both the start of the exponential phase and again at around 6h (Fig. 14B). In the *glcT* mutant, *prsS* is activated at the start of the exponential phase, however, it continues to be activated for up to 10h of growth (Fig. 14E). In the *sigB* mutant, *prsS* expression is activated primarily in stationary phase, unlike many other *prsS* repressors characterized (Fig. 14C).

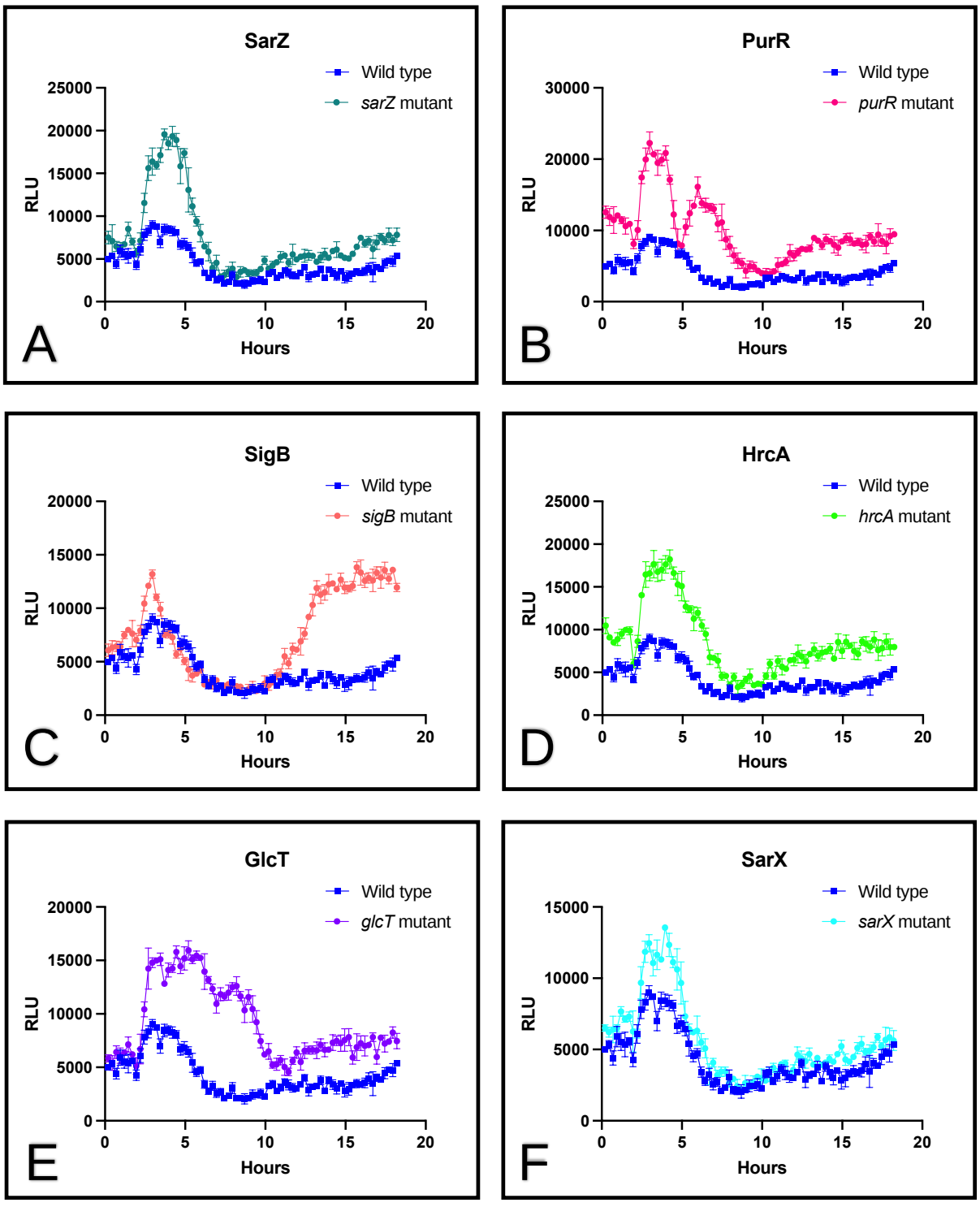

Figure 14. Validating factors responsible for repressing *prsS* expression. The pXEN1:P$_{prsS}$-*lux* plasmid was transduced into six USA300 LAC transcription factor mutant strains, as well as the wild type. The luminescence of each construct was measured in relative light units (RLU) over 18 hours. Each experiment was completed in biological triplicate, and error bars are shown representing ±SEM.

Validation of a *prsS* Activator

While only two potential activators of *prsS* expression were identified through our initial luciferase screens in the USA300 JE2 background (Fig. 11), our area under the curve analyses highlighted one potential activator as a point of interest - Rsp (Fig. 12). The *rsp* transcription factor mutant was transduced to a clean USA300 LAC background, to further validate that it was not only activating *prsS* promoter expression in JE2. After confirming both the *rsp* localized transposon and our transcriptional reporter fusion plasmid, our luciferase screen was performed again. This data shows that in the *rsp* mutant, *prsS* expression is slightly repressed suggesting that Rsp plays some role in activating *prsS* leading up to the exponential growth phase (Fig. 15). In the *rsp* mutant, *prsS* activity is primarily affected in the log growth phase, which is unique to our identified transcriptional regulators of *prsS* (Fig. 15).

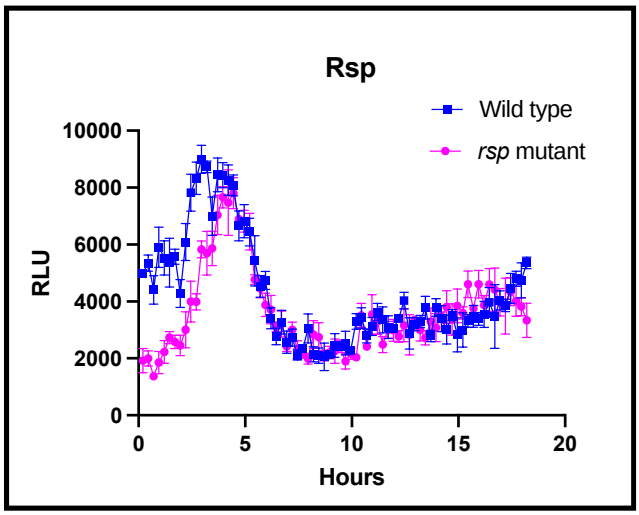

Figure 15. Rsp activates *prsS*. The pXEN1:*PprsS-lux* plasmid was placed into a USA300 LAC Rsp mutant as well as the wild type. The luminescence of these constructs was measured in relative light units (RLU) over 18 hours. This experiment was completed in biological triplicate, and error bars are shown representing ±SEM.

Discovery of a *prsS* Repressor Only Functional in the Presence of MMS

Because *prsS* expression is activated in the presence of DNA damage, we repeated our entire luciferase screen with over 100 transcription factor mutants in the presence of 1mM MMS to identify regulators that mediate such inducibility. These screens with MMS were initially performed in JE2, in which we identified one transcriptional factor mutant that displayed a substantial change in *prsS* expression when compared to our initial untreated screens. SrrA was identified as a moderate repressor of *prsS* activity in our untreated screens, however, in the treated *srrA* mutant, *prsS* expression is substantially activated. These observations were validated by transducing the *srrA* mutant to USA300 LAC, followed by our transcriptional reporter fusion and PCR confirmation. In Figure 16, we see that in the validated *srrA* mutant, *prsS* is activated during the exponential growth phase. Interestingly, *prsS* expression seems to be quickly repressed to wild-type levels, as this window of activation is only 2 hours.

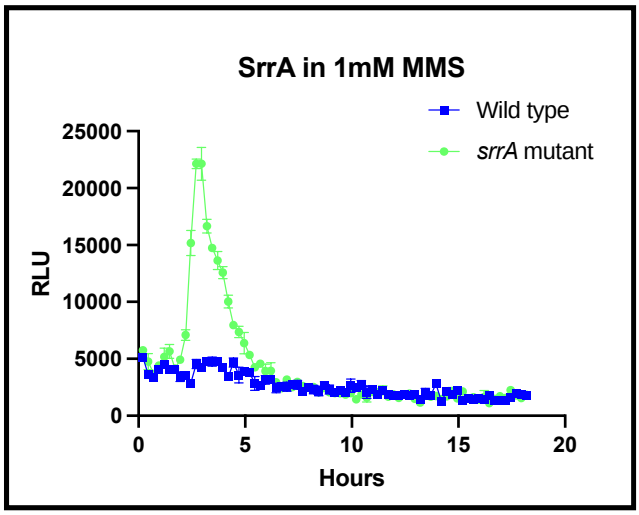

Figure 16. SrrA represses *prsS* in the presence of MMS. The pXEN1:P_{prsS}-*lux* plasmid was transduced into a USA300 LAC *srrA* mutant as well as the wild type. The luminescence of these constructs was measured in relative light units (RLU) over 18 hours while exposed to 1mM MMS. This experiment was completed in biological triplicate, and error bars are shown representing ±SEM.

Identification of PrsS Substrates Through N-Terminomics

In efforts to further characterize the role of the PrsS protease in *S. aureus* survival, stress response, and pathogenesis, we used N-terminomics methodologies to identify potential substrates of PrsS. We identified 29 substrates in the cytoplasmic (soluble) fraction (Table III), and 23 substrates in our membrane (insoluble) fraction (Table IV). To accomplish this, our *prsS* mutant strain was run alongside our wild type to determine which proteins were cleaved in the wild type but not in the mutant. By this process of elimination, we discovered 52 total substrates that were cleaved in the wild type and were not cleaved in the absence of PrsS. Each of these potential substrates gives us insight into PrsS' role in *S. aureus,* as these putative targets possess a wide range of cellular functions.

For example, it's clear that PrsS plays a role in the cleavage of proteins fundamental to protein synthesis. In terms of proteins that aid in translation, PrsS appears to cleave large ribosomal subunit proteins uL15, and uL2 which have fragments found in the cytoplasmic fraction (Table III), as well as uL2 and uL6 which have cleaved fragments found in the membrane fraction (Table IV). Additionally, PrsS cleaves one small ribosomal subunit protein – uS4 – of which cleaved fragments are found in the membrane fraction (Table IV). Aside from ribosomal subunits, other potential PrsS substrates that assist in translation and protein folding include elongation factor Tu (Table III), elongation factor Ts, DnaK, and ribosomal-associated chaperone trigger factor (Table IV). Interestingly, our data suggests that PrsS may cleave proteins PurB and ThrS which are involved in nucleotide biosynthesis (Table III, Table IV).

Table III. N-terminomics: Soluble Fraction

Protein Name	Gene	Locus tag
Nucleoid associated protein	-	SAUSA300_0453
Ornithine aminotransferase	*rocD*	SAUSA300_0860
Putative universal stress protein	-	SAUSA300_1656
Polyribonucleotide nucleotidyl trasnsferase	-	SAUSA300_0486
Cell division protein FtsZ	*ftsZ*	SAUSA300_1080
Phosphoribosylformylglycinamidine cyclo-ligase	*purM*	SAUSA300_0973
ATP-dependent Clp protease, ATP-binding subunit ClpC	*clpC*	SAUSA300_0515
Alkyl hydroperoxide reductase C	*ahpC*	SAUSA300_0380
Catalase	*katA*	SAUSA300_1232
Adenylosuccinate lyase	*purB*	SAUSA300_1889
Large ribosomal subunit protein uL15	*rplO*	SAUSA300_2185
UspA domain containing protein	-	SAUSA300_1652
Large ribosomal subunit protein uL2	*rplB*	SAUSA300_2201
Uncharacterized lipoprotein	-	SAUSA300_2315
Serine protease HtrA-like	-	SAUSA300_1674
Elastin binding protein EbpS	*ebpS*	SAUSA300_1370
Chaperone protein DnaK	*dnaK*	SAUSA300_1540
DHNA-CoA synthase	*menB*	SAUSA300_0948
Beta sliding clamp	*dnaN*	SAUSA300_0002
Threonine—tRNA ligase	*thrS*	SAUSA300_1629
FBP aldolase class I	*fda*	SAUSA300_2540
Phosphoglycerate kinase	*pgk*	SAUSA300_0757
Putative phosphoesterase	-	SAUSA300_0916
5’-nucelotidase family protein	-	SAUSA300_0025
Purine nucleoside phosphorylase DeoD-type	*deoD*	SAUSA300_2091
Peptidase M20 domain-containing protein 2	-	SAUSA300_2087
Probably malate:quinone oxidoreductase	*mqo*	SAUSA300_2541
Elongation factor Tu	*tuf*	SAUSA300_0533
UPF0342 protein	-	SAUSA300_1795

Table IV. N-terminomics: Insoluble Fraction

Protein Name	Gene	Locus tag
Large ribosomal subunit protein uL2	*rplB*	SAUSA300_2201
Large ribosomal subunit uL6	*rplF*	SAUSA300_2189
Uracil phosphoribosyltransferase	*upp*	SAUSA300_2066
Bacterial non-heme ferritin	*ftnA*	SAUSA300_1874
Small ribosomal subunit protein uS4	*rpsD*	SAUSA300_1666
Putative universal stress protein	-	SAUSA300_1656
Trigger factor	*tig*	SAUSA300_1622
Elastin binding protein EbpS	*ebpS*	SAUSA300_1370
Elongation factor Ts	*tsf*	SAUSA300_1150
Putative aldehyde dehydrogenase AldA	*aldA*	SAUSA300_0170
Dihydrocyacetone kinase DhaL	-	SAUSA300_0637
UspA domain containing protein	-	SAUSA300_1652
Serine protease HtrA-like	-	SAUSA300_1674
2,3-bisphosphoglycerate-independent phosphoglycerate mutase	*gpmI*	SAUSA300_0759
Succinate dehydrogenase	*sdhB*	SAUSA300_1048
Thioredoxin reductase	*trxB*	SAUSA300_0747
Alkaline shock response membrane anchor protein AmaP	-	SAUSA300_2144
ABC transporter, substrate-binding protein	-	SAUSA300_0618
Putative membrane protein	-	SAUSA300_2287
Uncharacterized protein	-	SAUSA300_2378
Maebl	-	SAUSA300_1684
Cell division protein FtsZ	*ftsZ*	SAUSA300_1080
Uncharacterized protein	-	SAUSA300_pUSA010004

Alternatively, many of these substrates contribute to *S. aureus'* stress response and defense, such as ClpC and AldA (Table III, Table IV). Aligning with the function of PrsS itself, this protease appears to target many stress response proteins that are linked to

oxidative conditions and metal ion regulation, including KatA, AhpC, TrxB, Mqo, and FtnA (Table III, Table IV). Our data also suggests that PrsS may cleave metabolic regulators like RocD (Table III). A final interesting target protein discovered through our N-terminomics experiments is the cell division protein FtsZ, as cleaved fragments are found in both the cytoplasmic and membrane fractions (Table III, Table IV).

CHAPTER FOUR: DISCUSSION

The M82s peptidases are a membrane-associated protease family that falls under a much larger superfamily of metallopeptidases [52]. This superfamily, called the MEM-family, contains a subfamily of G5 proteases (once known as type II CAAX Proteases and Bacteriocin Processing enzymes or CPBPs) encompassing more than 5,800 different proteins [24]. In a previous study, an alignment was made comparing the G5 proteins with other homologous protein families - including the M82 peptidases, DUF2324 (domain of unknown function), APH-1 (a γ-secretase subunit), and an unknown archaeal family - showing levels of metallopeptidase conservation across every kingdom of life [24]. The G5 proteins are defined in part by characteristics of this greater superfamily, including four core transmembrane domains, two conserved histidine residues, as well as two highly conserved glutamic acid residues [52,21,24]. An additional residue of interest, unique to G5 proteins and homologous families, is the variable aspartic acid/asparagine found in motif 4 [24].

A well-characterized G5 protein family member - Rce1 - is a protease found in *Saccharomyces cerevisiae* that requires this superfamily's hallmark glutamate and histidines for proteolytic function [53,21]. Additionally, Rce1 depends upon the aspartate in motif 4 for full catalytic activity [54]. Rce1 belongs to the COG1266 (cluster of orthologous groups) subfamily, which shares considerable resemblance to the COG2339

subfamily harboring the M82 peptidases [21,24]. The structural homology between these two families, in addition to the residue-specific loss of proteolytic activity in G5 proteins, inspired our investigation into the functional importance of these conserved protease motifs in M82 peptidases.

To date, publications exploring the functional importance of individual residues contributing to M82 peptidase proteolysis are scarce, as *B. subtilis* PrsW and *S. aureus* PrsS are the only members that have been evaluated in this way [21,23]. The founding member of the M82 peptidases, *B. subtilis* PrsW, is responsible for the site-1 proteolysis of an anti-sigma factor - RsiW; thus, immunoblotting for RsiW has been used as an indicator of PrsW proteolytic function [21]. Under NaOH-induced stress conditions, PrsW-mediated cleavage of RsiW results in the inhibition of this ASF's function [21]. However, upon alanine substitution of the conserved glutamate and histidine residues in this M82 protease, RsiW expression is returned, resulting in a loss of PrsW proteolytic activity [21].

Previous studies from our group show the functional importance of the conserved glutamic acid residues in *S. aureus* PrsS as well, in which alanine substitutions of these proposed catalytic residues exhibit reduced survival when exposed to DNA damage [23]. Here, our findings confirm that these glutamic acids, in addition to the histidine in motif 4, are necessary for proteolytic cleavage driven by PrsS. Interestingly, our western blot analyses suggest that the second conserved glutamic acid residue in PrsS (E216) may be necessary for PrsS protein formation entirely. It's possible that substituting this negatively charged glutamic acid with a small, non-polar alanine completely destabilizes

the PrsS protein [56,57]. While alanine substitutions are typically used to avoid altering main-chain protein conformation [58], there are plenty of examples in which these substitutions change both the core structure and protein stability across prokaryotes, eukaryotes, and viruses [59,60,61]. These observations in PrsS mirror what is observed in G5 protease *Saccharomyces cerevisiae* Rce1 [53], as well as fellow M82 peptidase PrsW, in that the functional loss of these residues conserved across the MEM-superfamily inhibit protease activity [53,21]; however, we also unveil that mutating these catalytic residues may impact overall protease stability.

In addition to conserved residues inherited from this large superfamily, our findings suggest that motifs specific to G5 proteins and homologous families may have a significant impact on M82 protease structure and function as well. The variable aspartate/asparagine residue in motif 4 is one of the most highly conserved motifs across these G5 homologs, following only behind the second glutamate and final histidine established by the MEM family in terms of conservation [24]. In the G5 protease Rce1, catalysis is partially impaired upon alanine substitution of its asparagine in this motif [55]. Alternatively, in multiple eukaryotic and archaeal homologs of Rce1, we see a completely abolished catalytic function when this Asp/Asn residue is alanine substituted [54,55]. While previous studies have described multiple prokaryotic G5 and M82 homologs as having an asparagine at this motif [24,62], our alignments show that this motif is occupied by an aspartate in *B. subtilis* PrsW, *C. difficile* PrsW, *S. aureus* PrsS, and a recently identified homolog in *L. brevis* [46]. Despite the highly conserved location of this motif, as well as the residue variability within individual protein families, to our knowledge, the

functional application of this residue has never been evaluated in M82 peptidases before this study. We observed that the alanine substitution of this aspartate in PrsS was unable to complement the wild-type response to DNA-damaging MMS, at a survival rate far worse than even the *prsS* mutant. This could be explained by an alteration in PrsS substrate selectivity at this residue, rather than the inability to cleave substrates, which has been documented previously in Rce1 orthologs [55]. By altering the substrate specificity of PrsS, this protease could potentially be cleaving things that are otherwise favorable to cell survival. While our OD_{600} readings of this aspartate substitution strain did not indicate any growth defect under standard conditions compared to the wild-type, this altered substrate specificity seems to be toxic only under MMS-induced stress conditions.

Evaluating the catalytic activity of the widely conserved M82 peptidases, as well as identifying their target substrates, is essential to further defining the functional roles of these proteases in bacterial survival and pathogenesis. As the objective of many new therapeutics involves targeting protease dysregulation [105], characterizing these proteolytic pathways is of high importance for treatment discovery as well. While the known M82 proteases operate through regulated intramembrane proteolysis-mediated release of an ECF sigma factor [65], reported substrates of this family to date only include anti-sigma factors [22,63]. Thus, the cellular roles of the M82 peptidases are typically characterized by their assistance in responding to external stress signals. However, through N-terminomics analyses of PrsS, we've uncovered that these peptidases likely play a much broader role in several important cellular functions including adhesion, protein folding, and cell division.

Our findings identified two substrates of PrsS that interact with the extracellular matrix (ECM) to facilitate adhesion to host tissues, including *S. aureus* elastin-binding protein and elongation factor Tu. The *S. aureus* Elastin-binding Protein (EbpS), binds to the N-terminal region of elastin fibers found on various host tissues, including the skin, lungs, and certain blood vessels, to facilitate adhesion [64,65]. As *ebpS* is also one of the primary genes that facilitates biofilm formation, it aids *S. aureus* in host colonization after host cells have been invaded [69]. Interestingly, while EbpS is exposed on the cell surface allowing this protein to bind to mammalian tissues, it is expressed as an integral membrane protein which explains the presence of this surface-presenting substrate within the insoluble fraction of our N-terminomics data [64]. Our findings demonstrate that PrsS cleaves EbpS at residue position 267, which is the precise location of a recombinant N-terminal truncate genetically engineered for a prior study [64]. This study showed that EbpS residues 1-267 are exposed on the cell surface and are targets for antibody binding [64]. This suggests that PrsS-mediated cleavage at this residue specifically targets EbpS affinity for host-cell binding and invasion by shedding EbpS from the cell surface [64]. As PrsS is activated in times of cellular stress [68], this protease may be preventing a mechanism intended to invade host cells and upregulate virulence factors to effectively manage this extracellular insult.

Another PrsS substrate, elongation factor Tu (EfTu), is a well-known facilitator of prokaryotic protein synthesis that moonlights in many different ways, including roles in cell-shape regulation, immune evasion and stimulation, and adhesion [66,67]. EfTu participates in adhesion by binding to proteins in the extracellular matrix of host cells and

has been observed to aid in *S. aureus* adhesion to keratinocytes through binding of Substance P [66,68]. Another primary way that EfTu participates in adhesion is by binding to heparin, commonly found on central venous catheters, resulting in *S. aureus* biofilm formation [74]. While EfTu is a known cell-surface target substrate, many fragmented variations of EfTu still contain functional heparin binding regions that allow biofilm formation to proceed [74]. Interestingly, our N-terminomics data indicates that PrsS seems to cleave EfTu at residue 272, which happens to be a previously characterized cleavage site [74]. This specific cleavage event is one of a few that creates a truncated version of the EfTu protein unable to bind to heparin, therefore inhibiting biofilm formation by this process [74]. PrsS may facilitate this cleavage to limit adhesion and biofilm formation in times of extracellular stress, so as not to remain stationary in an unfavorable environment. While this may seem counterintuitive as biofilms are often used for protective measures, there are examples of biofilm inhibition specifically in oxidative stress conditions [76]. It is also possible that PrsS cleaves adhesion proteins as a means to modulate excess virulence in times of stress.

Surprisingly, our findings indicate that PrsS also plays a role in the cleavage of *S. aureus* factors that support proliferation and protein folding, including FtsZ and DnaK. Generally, DnaK is needed to maintain a wealth of important cellular functions including stress tolerance, virulence, adhesion, and biofilm formation [70]. This Hsp70 family chaperone aids in protecting *S. aureus* from heat shock, oxidative, and antibiotic stress by folding and stabilizing select proteins while transferring damaged proteins to fellow chaperones for review [71]. This protein damage often happens during exposure to heat shock and

oxidative stress [71,72], where unfolded proteins are suspected to be the most susceptible to this proteotoxic stress [73]. The rate at which this continual binding and release of proteins occurs is dependent on interactions between the separate domains of DnaK: The N-terminal domain which is regulated by ATPase activity, and the C-terminal domain which binds substrates [75]. Notably, the ATP-bound state of the N-terminus results in a quick exchange of substrates, but the opposite is true for the ADP-bound state [75]. Our findings demonstrate that PrsS seemingly cleaves DnaK 57 residues from the N-terminal methionine, suggesting that this protease may be impacting the rate at which DnaK takes up proteins. While it remains unclear what effects this N-terminal cleavage of DnaK has on the cell, it's possible that substrate binding is slowed by PrsS interacting with the ATPase binding domain to preserve cellular energy for protective measures and core survival. Alternatively, PrsS could be altering this ATPase binding domain of DnaK as a housekeeping measure by moderating its activity until needed.

An additional protein of interest identified through our N-terminomics studies that assists in protein folding is the molecular chaperone trigger factor (TF) [77]. While TF is known to assist DnaK by protecting proteins from aggregating, and subsequently chaperoning proteins to the secretion system, it is not essential for survival nor required for *S. aureus* virulence [78,79]. In recent years, TF has been observed to cooperate with another *S. aureus* chaperone - PPIase enzyme PpiB - to assist in hemolysis and biofilm formation [79]. TF facilitates this cooperation through the use of three functional domains: a ribosomal binding domain, a central PPiase binding domain, and a chaperone domain [79]. Our findings show that this molecular chaperone does not appear to be cleaved

within any of these important domains, but instead appears to have only its N-terminal methionine removed. As the cleavage of this formyl-methionine is an event that occurs for every *S. aureus* protein upon maturation, we conclude that this cleavage event is likely not carried out by PrsS [97]. Instead, *S. aureus* contains a well-characterized peptide deformylase that hydrolyzes this methionine group, resulting in the methionine aminopeptidase-mediated removal of this amino acid [97]. This highlights the importance of immunoblotting potential substrates in future studies to validate our N-terminomics findings.

PrsS may also play a role in targeting cell division through the cleavage of protein FtsZ. FtsZ is a protein that facilitates the primary steps of cell division in Gram-positive organisms like *S. aureus*, as well as Gram-negative organisms, by aiding in the formation of the septal cell wall [80,81]. FtsZ facilitates this process by localizing to the divisome site, where it assembles into a ring of filamentous proteins and recruits enzymes that initiate peptidoglycan synthesis [81]. The process of continually binding peptidoglycan into successively smaller rings, ultimately dividing the cell, is driven by the GTPase activity of FtsZ [80,81]. The N-terminal domain of FtsZ carries out this GTPase activity by hydrolyzing nucleotides, thus keeping this protein in motion [82]. Our data suggests that PrsS cleaves FtsZ within the N-terminus, but outside of the GTP binding motif, immediately preceding leucine residue 69 [83]. While cleavage at this particular residue has not yet been analyzed in the literature, this leucine is conserved across *S. aureus, B. subtilis, E. coli, P. aeruginosa, M. tuberculosis, S. pneumoniae,* and *M. jannaschii,* indicating its importance [83]. Additionally, mutations of this leucine in *E.coli* have been

observed to reduce GTPase activity anywhere from 2 to 30 fold depending on the substitution [84,85]. This suggests that the PrsS-mediated cleavage at this residue may have a significant impact on GTPase activity. PrsS may cleave FtsZ at this location to reduce GTPase activity, therefore stalling proliferation in times of DNA damage. As cell division requires a substantial amount of energy and resources [86], it's possible that PrsS may participate in slowing down this process to preserve energy for stress response. However, a similar pathway inhibiting cell division in the presence of DNA damage has been characterized in *S. aureus*, indicating this may be what's occurring in PrsS engagement with FtsZ [96]. SosA is a protein that is activated in the presence of DNA damage, and ultimately seems to inhibit septal wall formation without altering FtsZ localization [96]. SosA appears to be regulated by a membrane protease, CtpA, as overexpression of SosA in a *ctpA* mutant renders cells no longer viable as a result of inhibited cell division [96]. Here, we predict that PrsS may be cleaving FtsZ directly reducing its GTPase activity, resulting in a similarly inhibitory effect [96].

To further evaluate the substrate specificity of PrsS, predicted cleavage sites of each putative substrate were compared to those of all other substrates with reference to the USA300 sample set. Five amino acids on either side of our identified cleavage site, found between P1' and P1, were individually analyzed for their percentage of differences to the sample set at each respective position. We found that PrsS possesses an affinity for substrates containing lysine, arginine, and alanine residues at the P1' position, with a reduced affinity for substrates containing leucine residues at P1' (Fig. 17). At the P2' position, this M82 protease appears to possess a greater affinity for substrates containing

arginine residues (Fig. 17). While there appear to be no residues of interest at positions P3' and P5' of putative PrsS substrates, we observed that this protease contains a preference for lysine residues at the P4' position (Fig. 17). Alternatively, PrsS appears to exhibit substrate recognition for either alanine or glycine at position P1 (Fig. 17). Other preferential substrate identification sites include either leucine or valine at the P2 position, however, no clear substrate specificity sites were determined for the P3 and P4 positions (Fig. 17). At position P5, we see that PrsS may possess an affinity for either a glycine or a proline residue (Fig. 17).

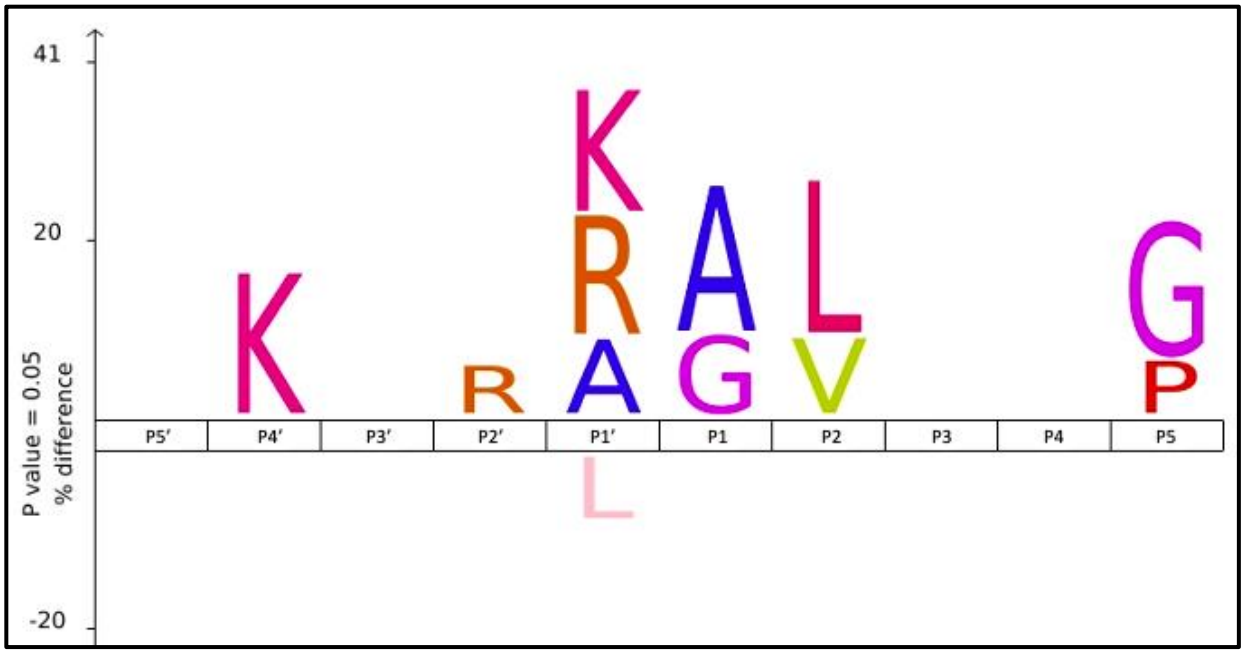

Figure 17. Substrate specificity of PrsS. The cleavage sites within each putative PrsS substrate were analyzed for their percentage of difference in frequency of amino acids at a given residue position. Five residues on either side of the start position for each substrate were evaluated using IceLogos.

While our N-terminomics data did not uncover an anti-sigma factor substrate linking PrsS to σ^S, repeating these studies under MMS-induced stress conditions may fill in this

knowledge gap. Nonetheless, our studies demonstrate a wealth of important cellular functions that are potentially impacted by this M82 peptidase. These findings highlight several questions and possibilities when it comes to this novel peptidase's role in adhesion, virulence modulation, protein folding, and proliferation. While it seems that PrsS may target its substrates in a manner that effectively optimizes *S. aureus* function in both the presence and absence of extracellular stress, it remains unclear what larger function the M82 peptidases possess beyond the scope of stress-induced ECF sigma-factor release. Through transcription-based analyses, we sought to further define the importance of this M82 peptidase within a larger regulatory network in both the presence and absence of an activating extracellular stress signal.

In our study, we found that the overwhelming majority of *S. aureus* transcription factors exhibit repressive effects on *prsS*, with only one activating exception. As *prsS* expression is activated by DNA-damaging and cell-wall targeting antimicrobial stress [7], it makes sense that this protease would be transcriptionally repressed until these stressors engage with the cell. One major repressor of *prsS* promoter activity is SarZ, which is a known global transcriptional regulator in *S. aureus*, upregulating the expression of a multitude of virulence factors and toxins [87]. In 2008, it was reported that SarZ played a role in the expression of roughly 87 genes; however, recent work suggests it is likely many more than this [88]. Importantly, SarZ promotes increased toxin production through upregulation of the *agr* system, resulting in an aggressive infection dynamic [87]. Due to this transcription factor's repression of biofilm formation and upregulation of toxins, it has been associated with dissemination stages of *S. aureus* infection [87,89]. Importantly,

SarZ is both a sensor and a regulator for oxidative stress via a cysteine (C-13) residue which influences gene regulation [86]. While PrsS has been established to assist in responding to oxidative stress [7], it's somewhat surprising that it would be repressed by an oxidative stress regulator. In the *sarZ* mutant, *prsS* is substantially upregulated, indicating this may be a compensatory tradeoff for circumventing oxidative stress. It's possible that SarZ, being a key virulence factor mediator, has more effective mechanisms by which it prepares for a response to oxidative stress [87]; however, in the *sarZ* mutant, it could be that *prsS* expression is activated as a backup in preparation for oxidative damage. Additionally, prior studies show that mutations in *sarZ* result in hypervirulent CA-MRSA bloodstream infections (BSI) [89]. As our group has previously observed PrsS to be advantageous in bloodstream infections [7], it's plausible that in the *sarZ* mutant, the expression of this protease is selected for to aid in BSI virulence and survival.

We see a similarly potential compensatory relationship between *prsS* expression and SrrA, however, this phenotype is only observed under DNA-damage-induced cellular stress. SrrA is another major transcriptional regulator in *S. aureus* and is part of a two-component system (SrrAB) known to facilitate oxidative and hypoxic stress regulation [90]. SrrAB is predicted to play a major role in the regulatory switch of *S. aureus* from the anaerobic to anaerobic lifestyle [91], and is well documented to regulate genes that protect the cell from external insult linked to oxidative damage [92,93]. Interestingly, this two-component system recognizes oxidative stress through a similar mechanism as SarZ, by use of a redox-sensitive cysteine [90]. SrrA represses *prsS* promoter activity in the presence of MMS, and likewise in the *srrA* mutant, *prsS* expression is significantly

upregulated. Given what we've seen with both SarZ and SrrA, it seems that PrsS may be used as a fail-safe in *S. aureus.* Upon the loss of major mediators of oxidative stress, *prsS* is activated and could possibly compensate for the lack of these regulators by initiating its own oxidative stress-response mechanism. However, because this repression of PrsS by SrrA is most clearly seen in the presence of DNA-damaging MMS, it's entirely possible that this two-component system could play a role in circumventing MMS-induced stress as well.

PurR is an additional major regulator of virulence factors and a repressor of *prsS* promoter activity [94]. PurR is primarily classified as a metabolic regulator of purine biosynthesis, however, it's been discovered to moonlight as a broad-spanning transcriptional regulator of virulence factors [95]. PurR binds to promoters of virulence factor genes directly, proving to be essential for the moderation of their expression [94]. In the *purR* mutant, *S. aureus* becomes hyperlethal and extremely cytotoxic, in part, through activation of SarA [94]. SarA activation then upregulates the *agr* system, resulting in significant Hla toxin production [95]. Additionally, the *purR* mutant is observed to upregulate protein A and fibronectin binding proteins, assisting this hypervirulent strain in biofilm formation [95]. As suggested by our N-terminomics data, PrsS appears to modulate adhesion and biofilm formation in a manner that inhibits these functions. Because *prsS* expression is activated in the *purR* mutant, it's possible that increased biofilm formation may be regulated by PrsS here as well.

A fellow repressor of *prsS* expression - SigB - is the primary stress response sigma factor in *S. aureus* [99]. This alternative sigma factor aids the cell in circumventing stress linked to acidic pH, excessive heat, glycopeptide and *β*-lactam antibiotics, and oxidation [100,101]. Importantly, *sigB* is primarily activated during the stationary growth phase [98], in which excess toxic iron and heightened levels of reactive oxygen species activate oxidative stress response mechanisms [102,103]. As the *sigB* mutant is substantially more susceptible to oxidative stress [100], gene expression during the stationary phase is vastly altered to prepare for growth-phase-specific threats [104]. Our findings demonstrate that in the *sigB* mutant, *prsS* expression is activated during the stationary phase, suggesting that this protease plays a role in *S. aureus* oxidative-stress response in both early and late growth stages. These findings are supported by prior studies by our group, in which wild-type *prsS* expression is greatest leading into the exponential phase [7], suggesting that stationary-phase activation of *prsS* is highly specific to the *sigB* mutant's heightened susceptibility to oxidative stress.

Interestingly, *prsS* expression is also repressed by HrcA, a heat-shock repression protein that negatively regulates Hsp family chaperones in the absence of stress [106]. This heat-shock repressor has been observed to cooperate with CstR, facilitating a dual repression of the *dnaK* and *groESL* operons that is unique to Staphylococci [106]. In the *hrcA* mutant, *prsS* expression is activated, which is interesting because PrsS may cleave DnaK in a manner that reduces the rate of protein folding activity; thus, it is possible that in the absence of HrcA, *prsS* is activated to take over repression of DnaK activity. As HrcA exhibits this repression in the absence of stress, it could be that PrsS acts as a

housekeeping protease by modulating DnaK activity when no extracellular stress is present.

The final major repressor of *prsS* expression identified in our transcription analyses is the transcriptional antiterminator GlcT [107]. While limited studies have been done on GlcT in *S. aureus,* prior research in *S. carnosus* indicates that this antiterminator functions as a metabolic regulator of glucose intake [108]. GlcT has been observed to act in a glucose-dependent manner, where in the presence of glucose, GlcT binds to the leader strand of glucose permease gene *ptsG* in a stabilizing conformation, allowing transcription and glucose intake [109]. However, in the absence of glucose, GlcT is inactivated and transcription is terminated [109]. It's possible that in the *glcT* mutant, PrsS is responsible for the cleavage and modulation of a glucose intake mechanism that, when unregulated, could be dangerous for the cell. However, it's also plausible that, similarly to PurR, GlcT may be primarily categorized as a metabolic regulator and could potentially moonlight as a major regulator of virulence factors in future studies.

The only activator, or rather non-repressor, of *prsS* expression observed in our findings is Rsp. Rsp, named for its role in the repression of surface proteins, is another transcription factor found to facilitate broad virulence factor regulation [110]. Like PurR, Rsp is observed to bind directly to promoters of virulence factors including the *hla, psma,* and *psmB* toxins, resulting in the activation of the *agr* system [110]. Activation of these toxins by Rsp is commonly associated with increased virulence in skin and soft tissue infections as well as pneumonia [110]. Additionally, Rsp is associated with inhibited

biofilm formation as it represses fibronectin binding proteins, as well as surface protein A, which is essential for biofilm production [111,112]. While many transcription factors exhibit repressive effects on *prsS* expression, Rsp seems to activate this protease. As *rsp* expression is induced by hydrogen peroxide, this factor may activate *prsS* to initiate a response to oxidative stress or assist in biofilm inhibition [113]. However, Rsp also controls a long non-coding RNA, SSR42, which influences the expression of virulence factors, including multiple toxins and surface proteins [114]. It could be that SSR42 influences *prsS* expression in an Rsp-dependent manner.

Through the identification of transcriptional regulators, potential substrates, and conserved homology required for catalytic function, we have further characterized the functional role of the M82 peptidases through the lens of PrsS. Our findings suggest that these proteases play a much larger role in complex cellular functions than previously thought. Here, we see that these peptidases seem to function through interaction with a large regulatory network of virulence factor modulators, impacting vital cellular functions such as proliferation, adhesion, protein folding, and biofilm formation. The M82 peptidases are able to do this through the use of a highly conserved protein structure that has been inherited over millennia, suggesting that many of these functions may be observed in PrsW homologs in future studies.

CHAPTER FIVE: FUTURE DIRECTIONS

In this study, multiple individual residues, as well as a single stretch of residues in the CTT of PrsS, were identified for their significance in stress response. It would be highly informative to further explore their role in protease function. The N-terminomics data obtained in this study provides potential substrates that can be used as indicators of PrsS cleavage. By performing western blots on these substrates in the wild type and *prsS* mutant, these cleavage events can be validated and further analyzed for their impact on cellular function. Additionally, performing these N-terminomics methods again with MMS induction could potentially identify a potential anti-sigma factor substrate of PrsS. This future experiment would be highly advantageous in identifying substrates of this protease that may only be cleaved in times of external stress. Further to this, evaluating the potential loss or gain of function specific to these substrates could provide greater detail on the larger role of PrsS in infection models, as many of our potential substrates impact factors that increase virulence in *S. aureus*.

In characterizing additional M82 homologs, alternative pathways may be discovered for sigma factor activation that provides clarity on the PrsS and SigS relationship. In this case, a wide range of future experiments could be used to evaluate the relationship between many of these uncharacterized homologs and their respective contribution to regulated intramembrane proteolysis within other gram-positive organisms.

REFERENCES

1. P R V, M J. A comparative analysis of community acquired and hospital acquired methicillin resistant Staphylococcus aureus. J Clin Diagn Res. 2013 Jul;7(7):1339-42. doi: 10.7860/JCDR/2013/5302.3139. Epub 2013 Jul 1. PMID: 23998061; PMCID: PMC3749631.

2. Harkins CP, Pichon B, Doumith M, Parkhill J, Westh H, Tomasz A, de Lencastre H, Bentley SD, Kearns AM, Holden MTG. Methicillin-resistant Staphylococcus aureus emerged long before the introduction of methicillin into clinical practice. Genome Biol. 2017 Jul 20;18(1):130. doi: 10.1186/s13059-017-1252-9. PMID: 28724393; PMCID: PMC5517843.

3. Giersing, B. K., Dastgheyb, S. S., Modjarrad, K., & Moorthy, V. (2016). Status of Vaccine Research and development of vaccines for Staphylococcus aureus. *Vaccine*, *34*(26), 2962–2966. https://doi.org/10.1016/j.vaccine.2016.03.110

4. Myles IA, Datta SK. Staphylococcus aureus: an introduction. Semin Immunopathol. 2012 Mar;34(2):181-4. doi: 10.1007/s00281-011-0301-9. Epub 2012 Jan 27. PMID: 22282052; PMCID: PMC3324845.

5. Kateete, D.P., Bwanga, F., Seni, J. *et al.* CA-MRSA and HA-MRSA coexist in community and hospital settings in Uganda. *Antimicrob Resist Infect Control* **8**, 94 (2019). https://doi.org/10.1186/s13756-019-0551-1

6. Saber H, Jasni AS, Jamaluddin TZMT, Ibrahim R. A Review of Staphylococcal Cassette Chromosome *mec* (SCC*mec*) Types in Coagulase-Negative Staphylococci (CoNS) Species. Malays J Med Sci. 2017 Oct;24(5):7-18. doi: 10.21315/mjms2017.24.5.2. Epub 2017 Oct 26. PMID: 29386968; PMCID: PMC5772811.

7. Bhatta DR, Cavaco LM, Nath G, Kumar K, Gaur A, Gokhale S, Bhatta DR. Association of Panton Valentine Leukocidin (PVL) genes with methicillin resistant Staphylococcus aureus (MRSA) in Western Nepal: a matter of concern for community infections (a hospital based prospective study). BMC Infect Dis. 2016 May 15;16:199. doi: 10.1186/s12879-016-1531-1. PMID: 27179682; PMCID: PMC4867903.

8. Tsouklidis N, Kumar R, Heindl SE, Soni R, Khan S. Understanding the Fight Against Resistance: Hospital-Acquired Methicillin-Resistant Staphylococcus Aureus vs. Community-Acquired Methicillin-Resistant Staphylococcus Aureus. Cureus. 2020 Jun 27;12(6):e8867. doi: 10.7759/cureus.8867. PMID: 32617248; PMCID: PMC7325383.

9. Gerlach, D., Guo, Y., De Castro, C. *et al.* Methicillin-resistant *Staphylococcus aureus* alters cell wall glycosylation to evade immunity. *Nature* 563, 705–709 (2018). https://doi.org/10.1038/s41586-018-0730-x

10. Clements, M. O., & Foster, S. J. (1999). Stress resistance in staphylococcus aureus. *Trends in Microbiology*, *7*(11), 458–462. https://doi.org/10.1016/s0966-842x(99)01607-8

11. Dastgheyb SS, Otto M. Staphylococcal adaptation to diverse physiologic niches: an overview of transcriptomic and phenotypic changes in different biological environments. Future Microbiol. 2015;10(12):1981-95. doi: 10.2217/fmb.15.116. Epub 2015 Nov 19. PMID: 26584249; PMCID: PMC4946774.

12. Arbade GK. Extra cytoplasmic sigma factors in Staphylococcus aureus ; their role and significance in the survival of Cocci. *J Appl Biotechnol Bioeng*. 2016;1(2):53-57. DOI: 10.15406/jabb.2016.01.00009

13. Rachel Anne Mooney, Seth A. Darst, Robert Landick. Sigma and RNA Polymerase: An On-Again, Off-Again Relationship?. Molecular Cell, Volume 20, Issue 3, 2005, Pages 335-345. ISSN 1097-2765, https://doi.org/10.1016/j.molcel.2005.10.015.

14. Campbell, E. A., Westblade, L. F., & Darst, S. A. (2008). Regulation of bacterial RNA polymerase σ factor activity: A structural perspective. *Current Opinion in Microbiology*, *11*(2), 121–127. https://doi.org/10.1016/j.mib.2008.02.016

15. Mascher, T. (2013). Signaling diversity and evolution of extracytoplasmic function (ECF) σ factors. *Current Opinion in Microbiology*, *16*(2), 148–155. https://doi.org/10.1016/j.mib.2013.02.001

16. Miller, H. K., Carroll, R. K., Burda, W. N., Krute, C. N., Davenport, J. E., & Shaw, L. N. (2012). The extracytoplasmic function sigma factor σ^{S}. *Journal of Bacteriology*, *194*(16), 4342–4354. https://doi.org/10.1128/jb.00484-12

17. Staroń A, Sofia HJ, Dietrich S, et al. The third pillar of bacterial signal transduction: classification of the extracytoplasmic function (ECF) sigma factor protein family. Molecular Microbiology. 2009 Nov;74(3):557-581. DOI: 10.1111/j.1365-2958.2009.06870.x. PMID: 19737356.

18. Hutchings MI, Hong HJ, Leibovitz E, Sutcliffe IC, Buttner MJ. The sigma(E) cell envelope stress response of Streptomyces coelicolor is influenced by a novel lipoprotein, CseA. J Bacteriol. 2006 Oct;188(20):7222-9. doi: 10.1128/JB.00818-06. Erratum in: J Bacteriol. 2008 Sep;190(17):6037. PMID: 17015661; PMCID: PMC1636229.

19. Wettstadt S, Llamas MA. Role of Regulated Proteolysis in the Communication of Bacteria With the Environment. Front Mol Biosci. 2020 Oct 15;7:586497. doi: 10.3389/fmolb.2020.586497. PMID: 33195433; PMCID: PMC7593790.

20. Janine Heinrich, Thomas Wiegert, Regulated intramembrane proteolysis in the control of extracytoplasmic function sigma factors. Research in Microbiology. Volume 160, Issue 9, 2009, Pages 696-703. ISSN 0923-2508, https://doi.org/10.1016/j.resmic.2009.08.019.

21. Ellermeier, C. D., & Losick, R. (2006). Evidence for a novel protease governing regulated intramembrane proteolysis and resistance to antimicrobial peptides in *bacillus subtilis*. *Genes & Development*, *20*(14), 1911–1922. https://doi.org/10.1101/gad.1440606

22. Ho, T. D., & Ellermeier, C. D. (2011). PRSW is required for colonization, resistance to antimicrobial peptides, and expression of extracytoplasmic function σ factors in clostridium difficile. *Infection and Immunity*, *79*(8), 3229–3238. https://doi.org/10.1128/iai.00019-11

23. Krute, C. N., Bell-Temin, H., Miller, H. K., Rivera, F. E., Weiss, A., Stevens, S. M., & Shaw, L. N. (2015). The membrane protein PRSS mimics σS in protecting Staphylococcus aureus against cell wall-targeting antibiotics and DNA-damaging agents. *Microbiology*, *161*(5), 1136–1148. https://doi.org/10.1099/mic.0.000065

24. Pei, J., Mitchell, D. A., Dixon, J. E., & Grishin, N. V. (2011). Expansion of type II caax proteases reveals evolutionary origin of γ-secretase subunit APH-1. *Journal of Molecular Biology*, *410*(1), 18–26. https://doi.org/10.1016/j.jmb.2011.04.066

25. International Working Group on the Classification of Staphylococcal Cassette Chromosome Elements (IWG-SCC). Classification of staphylococcal cassette chromosome mec (SCCmec): guidelines for reporting novel SCCmec elements. Antimicrob Agents Chemother. 2009 Dec;53(12):4961-7. doi: 10.1128/AAC.00579-09. Epub 2009 Aug 31. PMID: 19721075; PMCID: PMC2786320.

26. Ito T, Ma XX, Takeuchi F, Okuma K, Yuzawa H, Hiramatsu K. Novel type V staphylococcal cassette chromosome mec driven by a novel cassette chromosome recombinase, ccrC. Antimicrob Agents Chemother. 2004 Jul;48(7):2637-51. doi: 10.1128/AAC.48.7.2637-2651.2004. PMID: 15215121; PMCID: PMC434217.

27. Peng, H., Liu, D., Ma, Y. *et al.* Comparison of community- and healthcare-associated methicillin-resistant *Staphylococcus aureus* isolates at a Chinese tertiary hospital, 2012–2017. *Sci Rep* **8**, 17916 (2018). https://doi.org/10.1038/s41598-018-36206-5

28. Kwiecinski JM, Horswill AR. Staphylococcus aureus bloodstream infections: pathogenesis and regulatory mechanisms. Curr Opin Microbiol. 2020 Feb;53:51-60. doi: 10.1016/j.mib.2020.02.005. Epub 2020 Mar 12. PMID: 32172183; PMCID: PMC7244392.

29. Tong SY, Davis JS, Eichenberger E, Holland TL, Fowler VG Jr. Staphylococcus aureus infections: epidemiology, pathophysiology, clinical manifestations, and management. Clin Microbiol Rev. 2015 Jul;28(3):603-61. doi: 10.1128/CMR.00134-14. PMID: 26016486; PMCID: PMC4451395.

30. Ishii K, Adachi T, Yasukawa J, Suzuki Y, Hamamoto H, Sekimizu K. Induction of virulence gene expression in Staphylococcus aureus by pulmonary surfactant. Infect Immun. 2014 Apr;82(4):1500-10. doi: 10.1128/IAI.01635-13. Epub 2014 Jan 22. PMID: 24452679; PMCID: PMC3993393.

31. Nauta KM, Ho TD, Ellermeier CD. The Penicillin-Binding Protein PbpP Is a Sensor of β-Lactams and Is Required for Activation of the Extracytoplasmic Function σ Factor σ^P in Bacillus thuringiensis. mBio. 2021 Mar 23;12(2):e00179-21. doi: 10.1128/mBio.00179-21. PMID: 33758089; PMCID: PMC8092216.

32. Fuda CC, Fisher JF, Mobashery S. Beta-lactam resistance in Staphylococcus aureus: the adaptive resistance of a plastic genome. Cell Mol Life Sci. 2005 Nov;62(22):2617-33. doi: 10.1007/s00018-005-5148-6. PMID: 16143832.

33. Wong JW, Ip M, Tang A, Wei VW, Wong SY, Riley S, Read JM, Kwok KO. Prevalence and risk factors of community-associated methicillin-resistant *Staphylococcus aureus* carriage in Asia-Pacific region from 2000 to 2016: a systematic review and meta-analysis. Clin Epidemiol. 2018 Oct 12;10:1489-1501. doi: 10.2147/CLEP.S160595. PMID: 30349396; PMCID: PMC6190640.

34. Bleul L, Francois P, Wolz C. Two-Component Systems of *S. aureus*: Signaling and Sensing Mechanisms. Genes (Basel). 2021 Dec 23;13(1):34. doi: 10.3390/genes13010034. PMID: 35052374; PMCID: PMC8774646.

35. Wu, S., Lin, K., Liu, Y., Zhang, H., & Lei, L. (2020). Two-component signaling pathways modulate drug resistance of Staphylococcus aureus (Review). Biomedical Reports, 13, 5. https://doi.org/10.3892/br.2020.1312

36. Pané-Farré J, Jonas B, Förstner K, Engelmann S, Hecker M. The sigmaB regulon in Staphylococcus aureus and its regulation. Int J Med Microbiol. 2006 Aug;296(4-5):237-58. doi: 10.1016/j.ijmm.2005.11.011. Epub 2006 Apr 27. PMID: 16644280.

37. Walzl A, Marbach H, Belikova D, Vogl C, Ehling-Schulz M, Heilbronner S, Grunert T. Prevalence of the SigB-Deficient Phenotype among Clinical *Staphylococcus aureus* Isolates Linked to Bovine Mastitis. *Antibiotics*. 2023; 12(4):699. https://doi.org/10.3390/antibiotics12040699

38. Tuchscherr L, Bischoff M, Lattar SM, Noto Llana M, Pförtner H, Niemann S, Geraci J, Van de Vyver H, Fraunholz MJ, Cheung AL, Herrmann M, Völker U, Sordelli DO, Peters G, Löffler B. Sigma Factor SigB Is Crucial to Mediate Staphylococcus aureus Adaptation during Chronic Infections. PLoS Pathog. 2015 Apr 29;11(4):e1004870. doi: 10.1371/journal.ppat.1004870. PMID: 25923704; PMCID: PMC4414502.

39. Cordero, M., García-Fernández, J., Acosta, I.C. *et al.* The induction of natural competence adapts staphylococcal metabolism to infection. *Nat Commun* **13**, 1525 (2022). https://doi.org/10.1038/s41467-022-29206-7

40. Vitko NP, Grosser MR, Khatri D, Lance TR, Richardson AR. Expanded Glucose Import Capability Affords Staphylococcus aureus Optimized Glycolytic Flux during Infection. mBio. 2016 Jun 21;7(3):e00296-16. doi: 10.1128/mBio.00296-16. PMID: 27329749; PMCID: PMC4916373.

41. Shaw LN, Lindholm C, Prajsnar TK, Miller HK, Brown MC, Golonka E, Stewart GC, Tarkowski A, Potempa J. Identification and characterization of sigma, a novel component of the Staphylococcus aureus stress and virulence responses. PLoS One. 2008;3(12):e3844. doi: 10.1371/journal.pone.0003844. Epub 2008 Dec 3. PMID: 19050758; PMCID: PMC2585143.

42. Al Ali A, Alsulami J, Aubee JI, Idowu A, Tomlinson BR, Felton EA, Jackson JK, Kennedy SJ, Torres NJ, Shaw LN, Thompson KM. Staphylococcus aureus SigS Induces Expression of a Regulatory Protein Pair That Modulates Its mRNA Stability. J Bacteriol. 2023 Jun 27;205(6):e0039222. doi: 10.1128/jb.00392-22. Epub 2023 May 31. PMID: 37255480; PMCID: PMC10294688.

43. Fey PD, Endres JL, Yajjala VK, Widhelm TJ, Boissy RJ, Bose JL, Bayles KW. A genetic resource for rapid and comprehensive phenotype screening of nonessential Staphylococcus aureus genes. mBio. 2013 Feb 12;4(1):e00537-12. doi: 10.1128/mBio.00537-12. PMID: 23404398; PMCID: PMC3573662.

44. Weiss A, Jackson JK, Shaw LN, Skaar EP. Screening transcriptional connections in *Staphylococcus aureus* using high-throughput transduction of bioluminescent reporter plasmids. Microbiology (Reading). 2022 Apr;168(4):001174. doi: 10.1099/mic.0.001174. PMID: 35446249; PMCID: PMC10233262.

45. Neil D Rawlings, Alan J Barrett, Paul D Thomas, Xiaosong Huang, Alex Bateman, Robert D Finn, The *MEROPS* database of proteolytic enzymes, their substrates and inhibitors in 2017 and a comparison with peptidases in the PANTHER database, *Nucleic Acids Research*, Volume 46, Issue D1, 4 January 2018, Pages D624–D632, https://doi.org/10.1093/nar/gkx1134

46. The UniProt Consortium , UniProt: the Universal Protein Knowledgebase in 2023, *Nucleic Acids Research*, Volume 51, Issue D1, 6 January 2023, Pages D523–D531, https://doi.org/10.1093/nar/gkac1052

47. Salisbury V, Hedges RW, Datta N. Two modes of "curing" transmissible bacterial plasmids. J Gen Microbiol. 1972 May;70(3):443-52. doi: 10.1099/00221287-70-3-443. PMID: 4556250.

48. Highlander SK, Hultén KG, Qin X, Jiang H, Yerrapragada S, Mason EO Jr, Shang Y, Williams TM, Fortunov RM, Liu Y, Igboeli O, Petrosino J, Tirumalai M, Uzman A, Fox GE, Cardenas AM, Muzny DM, Hemphill L, Ding Y, Dugan S, Blyth PR, Buhay CJ, Dinh HH, Hawes AC, Holder M, Kovar CL, Lee SL, Liu W, Nazareth LV, Wang Q, Zhou J, Kaplan SL, Weinstock GM. Subtle genetic changes enhance virulence of methicillin resistant and sensitive Staphylococcus aureus. BMC Microbiol. 2007 Nov 6;7:99. doi: 10.1186/1471-2180-7-99. PMID: 17986343; PMCID: PMC2222628.

49. Sullivan MA, Yasbin RE, Young FE. New shuttle vectors for Bacillus subtilis and Escherichia coli which allow rapid detection of inserted fragments. Gene. 1984 Jul-Aug;29(1-2):21-6. doi: 10.1016/0378-1119(84)90161-6. PMID: 6092222.

50. Francis KP, Joh D, Bellinger-Kawahara C, Hawkinson MJ, Purchio TF, Contag PR. Monitoring bioluminescent Staphylococcus aureus infections in living mice using a novel luxABCDE construct. Infect Immun. 2000 Jun;68(6):3594-600. doi: 10.1128/IAI.68.6.3594-3600.2000. PMID: 10816517; PMCID: PMC97648.

51. Protter: interactive protein feature visualization and integration with experimental proteomic data. Omasits U, Ahrens CH, Müller S, Wollscheid B. Bioinformatics. 2014 Mar 15;30(6):884-6. doi: 10.1093/bioinformatics/btt607.

52. Pei J., Grishin N.V. Type II CAAX prenyl endopeptidases belong to a novel superfamily of putative membrane-bound metalloproteases. *Trends Biochem. Sci.* 2001;26:275.

53. Dolence J.M., Steward L.E., Dolence E.K., Wong D.H., Poulter C.D. Studies with recombinant *Saccharomyces cerevisiae* CaaX prenyl protease Rce1p. *Biochemistry.* 2000;39:4096–4104

54. Manolaridis I, Kulkarni K, Dodd RB, Ogasawara S, Zhang Z, Bineva G, Reilly NO, Hanrahan SJ, Thompson AJ, Cronin N, Iwata S, Barford D. Mechanism of farnesylated CAAX protein processing by the intramembrane protease Rce1. Nature. 2013 Dec 12;504(7479):301-5. doi: 10.1038/nature12754. Epub 2013 Dec 1. PMID: 24291792; PMCID: PMC3864837.

55. Plummer LJ, Hildebrandt ER, Porter SB, Rogers VA, McCracken J, Schmidt WK. Mutational analysis of the ras converting enzyme reveals a requirement for glutamate and histidine residues. J Biol Chem. 2006 Feb 24;281(8):4596-605. doi: 10.1074/jbc.M506284200. Epub 2005 Dec 17. PMID: 16361710; PMCID: PMC2937830.

56. Biro JC. Amino acid size, charge, hydropathy indices and matrices for protein structure analysis. Theor Biol Med Model. 2006 Mar 22;3:15. doi: 10.1186/1742-4682-3-15. PMID: 16551371; PMCID: PMC1450267.

57. Bischoff, R., & Schlüter, H. (2012). Amino acids: chemistry, functionality and selected non-enzymatic post-translational modifications. *Journal of proteomics*, *75*(8), 2275-2296.

58. Fabrice Lefèvre, Marie-Hélène Rémy, Jean-Michel Masson, Alanine-stretch scanning mutagenesis: a simple and efficient method to probe protein structure and function, *Nucleic Acids Research*, Volume 25, Issue 2, 1 January 1997, Pages 447–448, https://doi.org/10.1093/nar/25.2.447

59. Nathaniel D. M. Holman, Anthony J. Wilkinson, Margaret C. M. Smith. Alanine-scanning mutagenesis of protein mannosyl-transferase from Streptomyces coelicolor reveals strong activity-stability correlation. Microbiology, vol. 167, issue 10, (2021), pp: 001103, Published by Microbiology Society.

60. Murray CL, Jones CT, Tassello J, Rice CM. Alanine scanning of the hepatitis C virus core protein reveals numerous residues essential for production of infectious virus. J Virol. 2007 Oct;81(19):10220-31. doi: 10.1128/JVI.00793-07. Epub 2007 Jul 18. PMID: 17634240; PMCID: PMC2045476.

61. Lee SY, Pullen L, Virgil DJ, Castañeda CA, Abeykoon D, Bolon DN, Fushman D. Alanine scan of core positions in ubiquitin reveals links between dynamics, stability, and function. J Mol Biol. 2014 Apr 3;426(7):1377-89. doi: 10.1016/j.jmb.2013.10.042. Epub 2013 Dec 19. PMID: 24361330; PMCID: PMC3951674.

62. Kjos M, Snipen L, Salehian Z, Nes IF, Diep DB. The abi proteins and their involvement in bacteriocin self-immunity. J Bacteriol. 2010 Apr;192(8):2068-76. doi: 10.1128/JB.01553-09. Epub 2010 Feb 12. PMID: 20154137; PMCID: PMC2849437.

63. Heinrich J, Hein K, Wiegert T. Two proteolytic modules are involved in regulated intramembrane proteolysis of Bacillus subtilis RsiW. Mol Microbiol. 2009 Dec;74(6):1412-26. doi: 10.1111/j.1365-2958.2009.06940.x. Epub 2009 Nov 2. PMID: 19889088.

64. Downer R, Roche F, Park PW, Mecham RP, Foster TJ. The elastin-binding protein of Staphylococcus aureus (EbpS) is expressed at the cell surface as an integral membrane protein and not as a cell wall-associated protein. J Biol Chem. 2002 Jan 4;277(1):243-50. doi: 10.1074/jbc.M107621200. Epub 2001 Oct 29. PMID: 11684686.

65. Kot B, Sytykiewicz H, Sprawka I. Expression of the Biofilm-Associated Genes in Methicillin-Resistant *Staphylococcus aureus* in Biofilm and Planktonic Conditions. Int J Mol Sci. 2018 Nov 6;19(11):3487. doi: 10.3390/ijms19113487. PMID: 30404183; PMCID: PMC6274806.

66. Harvey KL, Jarocki VM, Charles IG, Djordjevic SP. The Diverse Functional Roles of Elongation Factor Tu (EF-Tu) in Microbial Pathogenesis. Front Microbiol. 2019 Oct 24;10:2351. doi: 10.3389/fmicb.2019.02351. PMID: 31708880; PMCID: PMC6822514.

67. Morse, J. C. et al. Elongation factor-Tu can repetitively engage aminoacyl-tRNA within the ribosome during the proofreading stage of tRNA selection. *Proc. Natl Acad. Sci. USA* 117, 3610–3620 (2020).

68. N'Diaye A, Mijouin L, Hillion M, Diaz S, Konto-Ghiorghi Y, Percoco G, Chevalier S, Lefeuvre L, Harmer NJ, Lesouhaitier O, Feuilloley MG. Effect of Substance P in Staphylococcus aureus and Staphylococcus epidermidis Virulence: Implication for Skin Homeostasis. Front Microbiol. 2016 Apr 15;7:506. doi: 10.3389/fmicb.2016.00506. PMID: 27148195; PMCID: PMC4832252.

69. Idrees M, Sawant S, Karodia N, Rahman A. *Staphylococcus aureus* Biofilm: Morphology, Genetics, Pathogenesis and Treatment Strategies. Int J Environ Res Public Health. 2021 Jul 16;18(14):7602. doi: 10.3390/ijerph18147602. PMID: 34300053; PMCID: PMC8304105.

70. V.K. Singh, M. Syring, A. Singh, *et al.* An insight into the significance of the DnaK heat shock system in *Staphylococcus aureus.* Int J Med Microbiol, 302 (6) (2012), pp. 242-252, 10.1016/j.ijmm.2012.05.001. PMid: 22748508

71. Fay, A., & Glickman, M. S. (2014). An essential nonredundant role for mycobacterial DnaK in native protein folding. *PLoS genetics*, *10*(7), e1004516.

72. Paull TT. DNA damage and regulation of protein homeostasis. DNA Repair (Amst). 2021 Sep;105:103155. doi: 10.1016/j.dnarep.2021.103155. Epub 2021 Jun 8. PMID: 34116476; PMCID: PMC8364502.

73. Santra M, Dill KA, de Graff AMR. How Do Chaperones Protect a Cell's Proteins from Oxidative Damage? Cell Syst. 2018 Jun 27;6(6):743-751.e3. doi: 10.1016/j.cels.2018.05.001. Epub 2018 Jun 6. PMID: 29886110.

74. Widjaja M, Harvey KL, Hagemann L, Berry IJ, Jarocki VM, Raymond BBA, Tacchi JL, Gründel A, Steele JR, Padula MP, Charles IG, Dumke R, Djordjevic SP. Elongation factor Tu is a multifunctional and processed moonlighting protein. Sci Rep. 2017 Sep 11;7(1):11227. doi: 10.1038/s41598-017-10644-z. PMID: 28894125; PMCID: PMC5593925.

75. Zhu X, Zhao X, Burkholder WF, Gragerov A, Ogata CM, Gottesman ME, Hendrickson WA. Structural analysis of substrate binding by the molecular chaperone DnaK. Science. 1996 Jun 14;272(5268):1606-14. doi: 10.1126/science.272.5268.1606. PMID: 8658133; PMCID: PMC5629921.

76. Gozzi, K., Ching, C., Paruthiyil, S. *et al. Bacillus subtilis* utilizes the DNA damage response to manage multicellular development. *npj Biofilms Microbiomes* 3, 8 (2017). https://doi.org/10.1038/s41522-017-0016-3

77. Deuerling, E., Schulze-Specking, A., Tomoyasu, T. *et al.* Trigger factor and DnaK cooperate in folding of newly synthesized proteins. *Nature* 400, 693–696 (1999). https://doi.org/10.1038/23301

78. Agashe V.R., Guha S., Chang H.C., Genevaux P., Hayer-Hartl M., Stemp M., Georgopoulos C., Hartl F.U., Barral J.M. Function of trigger factor and DnaK in multidomain protein folding: increase in yield at the expense of folding speed. *Cell.* 2004; 117: 199-209.

79. Kramer G, Patzelt H, Rauch T, Kurz TA, Vorderwülbecke S, Bukau B, Deuerling E. Trigger factor peptidyl-prolyl cis/trans isomerase activity is not essential for the folding of cytosolic proteins in Escherichia coli. J Biol Chem. 2004 Apr 2;279(14):14165-70. doi: 10.1074/jbc.M313635200. Epub 2004 Jan 16. PMID: 14729669.

80. Huecas S, Canosa-Valls AJ, Araújo-Bazán L, Ruiz FM, Laurents DV, Fernández-Tornero C, Andreu JM. Nucleotide-induced folding of cell division protein FtsZ from Staphylococcus aureus. FEBS J. 2020 Sep;287(18):4048-4067. doi: 10.1111/febs.15235. Epub 2020 Feb 24. PMID: 31997533.

81. Bisson-Filho AW, Hsu YP, Squyres GR, Kuru E, Wu F, Jukes C, Sun Y, Dekker C, Holden S, VanNieuwenhze MS, Brun YV, Garner EC. Treadmilling by FtsZ filaments drives peptidoglycan synthesis and bacterial cell division. Science. 2017 Feb 17;355(6326):739-743. doi: 10.1126/science.aak9973. Erratum in: Science. 2020 Jan 17;367(6475): PMID: 28209898; PMCID: PMC5485650.

82. N. Silber, C.L. Matos de Opitz, C. Mayer, P. Sass. Cell division protein FtsZ: from structure and mechanism to antibiotic target. Future Microbiol., 15 (2020), pp. 801-831, 10.2217/fmb-2019-0348

83. Rachana Rao Battaje, Ravikant Piyush, Vidyadhar Pratap, Dulal Panda; Models versus pathogens: how conserved is the FtsZ in bacteria?. *Biosci Rep* 27 February 2023; 43 (2): BSR20221664. doi: https://doi.org/10.1042/BSR20221664

84. Blasios V., Bisson-Filho A.W., Castellen P., Nogueira M.L.C., Bettini J., Portugal R.V. et al. (2013) Genetic and biochemical characterization of the MinC-FtsZ interaction in Bacillus subtilis. *PloS ONE* 8, e60690[PubMed] https://doi.org/10.1371/journal.pone.0060690

85. Redick SD, Stricker J, Briscoe G, Erickson HP (2005) Mutants of FtsZ targeting the protofilament interface: effects on cell division and GTPase activity. J. Bacteriol. 187: 2727–2736.

86. Salazar-Roa M, Malumbres M. Fueling the Cell Division Cycle. Trends Cell Biol. 2017 Jan;27(1):69-81. doi: 10.1016/j.tcb.2016.08.009. Epub 2016 Oct 13. PMID: 27746095.

87. Tamber S, Cheung AL. SarZ promotes the expression of virulence factors and represses biofilm formation by modulating SarA and agr in Staphylococcus aureus. Infect Immun. 2009 Jan;77(1):419-28. doi: 10.1128/IAI.00859-08. Epub 2008 Oct 27. PMID: 18955469; PMCID: PMC2612251.

88. Chen, P.R.; Nishida, S.; Poor, C.B.; Cheng, A.; Bae, T.; Kuechenmeister, L.; Dunman, P.M.; Missiakas, D.; He, C. A new oxidative sensing and regulation pathway mediated by the MgrA homologue SarZ in *Staphylococcus aureus*. *Mol. Microbiol.* 2009, *71*, 198–211.

89. Dyzenhaus S, Sullivan MJ, Alburquerque B, Boff D, van de Guchte A, Chung M, Fulmer Y, Copin R, Ilmain JK, O'Keefe A, Altman DR, Stubbe FX, Podkowik M, Dupper AC, Shopsin B, van Bakel H, Torres VJ. MRSA lineage USA300 isolated from bloodstream infections exhibit altered virulence regulation. Cell Host Microbe. 2023 Feb 8;31(2):228-242.e8. doi: 10.1016/j.chom.2022.12.003. Epub 2023 Jan 20. PMID: 36681080; PMCID: PMC9911362.

90. Tiwari, N.; López-Redondo, M.; Miguel-Romero, L.; Kulhankova, K.; Cahill, M.P.; Tran, P.M.; Kinney, K.J.; Kilgore, S.H.; Al-Tameemi, H.; Herfst, C.A. The SrrAB two-component system regulates *Staphylococcus aureus* pathogenicity through redox sensitive cysteines. *Proc. Natl. Acad. Sci. USA* 2020, *117*, 10989–10999.

91. Kinkel TL, Roux CM, Dunman PM, Fang FC. The Staphylococcus aureus SrrAB two-component system promotes resistance to nitrosative stress and hypoxia. mBio. 2013 Nov 12;4(6):e00696-13. doi: 10.1128/mBio.00696-13. PMID: 24222487; PMCID: PMC3892780.

92. Windham IH, Chaudhari SS, Bose JL, Thomas VC, Bayles KW. SrrAB Modulates Staphylococcus aureus Cell Death through Regulation of cidABC Transcription. J Bacteriol. 2016 Jan 25;198(7):1114-22. doi: 10.1128/JB.00954-15. PMID: 26811317; PMCID: PMC4800867.

93. Mashruwala AA, Boyd JM. The Staphylococcus aureus SrrAB Regulatory System Modulates Hydrogen Peroxide Resistance Factors, Which Imparts Protection to Aconitase during Aerobic Growth. PLoS One. 2017 Jan 18;12(1):e0170283. doi: 10.1371/journal.pone.0170283. PMID: 28099473; PMCID: PMC5242492.

94. Sause WE, Balasubramanian D, Irnov I, Copin R, Sullivan MJ, Sommerfield A, Chan R, Dhabaria A, Askenazi M, Ueberheide B, Shopsin B, van Bakel H, Torres VJ. The purine biosynthesis regulator PurR moonlights as a virulence regulator in *Staphylococcus aureus*. Proc Natl Acad Sci U S A. 2019 Jul 2;116(27):13563-13572. doi: 10.1073/pnas.1904280116. Epub 2019 Jun 19. PMID: 31217288; PMCID: PMC6613142.

95. Alkam D, Jenjaroenpun P, Ramirez AM, Beenken KE, Spencer HJ, Smeltzer MS. The Increased Accumulation of Staphylococcus aureus Virulence Factors Is Maximized in a *purR* Mutant by the Increased Production of SarA and Decreased Production of Extracellular Proteases. Infect Immun. 2021 Mar 17;89(4):e00718-20. doi: 10.1128/IAI.00718-20. PMID: 33468580; PMCID: PMC8090970.

96. Bojer MS, Wacnik K, Kjelgaard P, Gallay C, Bottomley AL, Cohn MT, Lindahl G, Frees D, Veening JW, Foster SJ, Ingmer H. SosA inhibits cell division in Staphylococcus aureus in response to DNA damage. Mol Microbiol. 2019 Oct;112(4):1116-1130. doi: 10.1111/mmi.14350. Epub 2019 Aug 16. PMID: 31290194; PMCID: PMC6851548.

97. Lewandowski T, Huang J, Fan F, Rogers S, Gentry D, Holland R, Demarsh P, Aubart K, Zalacain M. Staphylococcus aureus formyl-methionyl transferase mutants demonstrate reduced virulence factor production and pathogenicity. Antimicrob Agents Chemother. 2013 Jul;57(7):2929-36. doi: 10.1128/AAC.00162-13. Epub 2013 Apr 9. PMID: 23571548; PMCID: PMC3697361.

98. Supa-Amornkul S, Mongkolsuk P, Summpunn P, Chaiyakunvat P, Navaratdusit W, Jiarpinitnun C, Chaturongakul S. Alternative Sigma Factor B in Bovine Mastitis-Causing *Staphylococcus aureus*: Characterization of Its Role in Biofilm Formation, Resistance to Hydrogen Peroxide Stress, Regulon Members. Front Microbiol. 2019 Nov 7;10:2493. doi: 10.3389/fmicb.2019.02493. PMID: 31787937; PMCID: PMC6853994.

99. Anderson KL, Roberts C, Disz T, Vonstein V, Hwang K, Overbeek R, Olson PD, Projan SJ, Dunman PM. Characterization of the Staphylococcus aureus heat shock, cold shock, stringent, and SOS responses and their effects on log-phase mRNA turnover. J Bacteriol. 2006 Oct;188(19):6739-56. doi: 10.1128/JB.00609-06. PMID: 16980476; PMCID: PMC1595530.

100. Davis AO, O'Leary JO, Muthaiyan A, Langevin MJ, Delgado A, Abalos AT, Fajardo AR, Marek J, Wilkinson BJ, Gustafson JE. Characterization of Staphylococcus aureus mutants expressing reduced susceptibility to common house-cleaners. J Appl Microbiol. 2005;98(2):364-72. doi: 10.1111/j.1365-2672.2004.02460.x. PMID: 15659191; PMCID: PMC3552489.

101. Ranganathan N, Johnson R, Edwards AM. The general stress response of *Staphylococcus aureus* promotes tolerance of antibiotics and survival in whole human blood. Microbiology (Reading). 2020 Nov;166(11):1088-1094. doi: 10.1099/mic.0.000983. Epub 2020 Oct 23. PMID: 33095698; PMCID: PMC7723259.

102. Fritsch VN, Loi VV, Busche T, Tung QN, Lill R, Horvatek P, Wolz C, Kalinowski J, Antelmann H. The alarmone (p)ppGpp confers tolerance to oxidative stress during the stationary phase by maintenance of redox and iron homeostasis in Staphylococcus aureus. Free Radic Biol Med. 2020 Dec;161:351-364. doi: 10.1016/j.freeradbiomed.2020.10.322. Epub 2020 Nov 1. PMID: 33144262; PMCID: PMC7754856.

103. Hammer ND, Skaar EP. Molecular mechanisms of Staphylococcus aureus iron acquisition. Annu Rev Microbiol. 2011;65:129-47. doi: 10.1146/annurev-micro-090110-102851. PMID: 21639791; PMCID: PMC3807827.

104. Andy Weiss, William H. Broach, Lindsey N. Shaw, Characterizing the transcriptional adaptation of *Staphylococcus aureus* to stationary phase growth, *Pathogens and Disease*, Volume 74, Issue 5, July 2016, ftw046, https://doi.org/10.1093/femspd/ftw046

105. Bleuez C, Koch WF, Urbach C, Hollfelder F, Jermutus L. Exploiting protease activation for therapy. Drug Discov Today. 2022 Jun;27(6):1743-1754. doi: 10.1016/j.drudis.2022.03.011. Epub 2022 Mar 18. PMID: 35314338; PMCID: PMC9132161.

106. Chastanet A, Fert J, Msadek T. Comparative genomics reveal novel heat shock regulatory mechanisms in Staphylococcus aureus and other Gram-positive bacteria. Mol Microbiol. 2003 Feb;47(4):1061-73. doi: 10.1046/j.1365-2958.2003.03355.x. PMID: 12581359.

107. Thomas Geissmann, Clément Chevalier, Marie-Josée Cros, Sandrine Boisset, Pierre Fechter, Céline Noirot, Jacques Schrenzel, Patrice François, François Vandenesch, Christine Gaspin, Pascale Romby, A search for small noncoding RNAs in *Staphylococcus aureus* reveals a conserved sequence motif for regulation, *Nucleic Acids Research*, Volume 37, Issue 21, 1 November 2009, Pages 7239–7257, https://doi.org/10.1093/nar/gkp668

108. Knezevic I, Bachem S, Sickmann A, Meyer HE, Stülke J, Hengstenberg W. Regulation of the glucose-specific phosphotransferase system (PTS) of Staphylococcus carnosus by the antiterminator protein GlcT. Microbiology (Reading). 2000 Sep;146 (Pt 9):2333-2342. doi: 10.1099/00221287-146-9-2333. PMID: 10974121.

109. Santangelo TJ, Artsimovitch I. Termination and antitermination: RNA polymerase runs a stop sign. Nat Rev Microbiol. 2011 May;9(5):319-29. doi: 10.1038/nrmicro2560. Epub 2011 Apr 11. PMID: 21478900; PMCID: PMC3125153.

110. Liu B, Sun B. Rsp promotes the transcription of virulence factors in an *agr*-independent manner in *Staphylococcus aureus*. Emerg Microbes Infect. 2020 Dec;9(1):796-812. doi: 10.1080/22221751.2020.1752116. PMID: 32248753; PMCID: PMC7241556.

111. Lei MG, Cue D, Roux CM, Dunman PM, Lee CY. Rsp inhibits attachment and biofilm formation by repressing fnbA in Staphylococcus aureus MW2. J Bacteriol. 2011 Oct;193(19):5231-41. doi: 10.1128/JB.05454-11. Epub 2011 Jul 29. PMID: 21804010; PMCID: PMC3187379.

112. Archer NK, Mazaitis MJ, Costerton JW, Leid JG, Powers ME, Shirtliff ME. Staphylococcus aureus biofilms: properties, regulation, and roles in human disease. Virulence. 2011 Sep-Oct;2(5):445-59. doi: 10.4161/viru.2.5.17724. Epub 2011 Sep 1. PMID: 21921685; PMCID: PMC3322633.

113. Das S, Lindemann C, Young BC, Muller J, Österreich B, Ternette N, Winkler AC, Paprotka K, Reinhardt R, Förstner KU, Allen E, Flaxman A, Yamaguchi Y, Rollier CS, van Diemen P, Blättner S, Remmele CW, Selle M, Dittrich M, Müller T, Vogel J, Ohlsen K, Crook DW, Massey R, Wilson DJ, Rudel T, Wyllie DH, Fraunholz MJ. Natural mutations in a Staphylococcus aureus virulence regulator attenuate cytotoxicity but permit bacteremia and abscess formation. Proc Natl Acad Sci U S A. 2016 May 31;113(22):E3101-10. doi: 10.1073/pnas.1520255113. Epub 2016 May 16. PMID: 27185949; PMCID: PMC4896717.

114. Morrison JM, Miller EW, Benson MA, Alonzo F 3rd, Yoong P, Torres VJ, Hinrichs SH, Dunman PM. Characterization of SSR42, a novel virulence factor regulatory RNA that contributes to the pathogenesis of a Staphylococcus aureus USA300 representative. J Bacteriol. 2012 Jun;194(11):2924-38. doi: 10.1128/JB.06708-11. Epub 2012 Apr 6. PMID: 22493015; PMCID: PMC3370614.

115. Colaert N, Helsens K, Martens L, Vandekerckhove J, Gevaert K. Improved visualization of protein consensus sequences by iceLogo. Nat Methods. 2009 Nov;6(11):786-7. doi: 10.1038/nmeth1109-786. PMID: 19876014.